Holocene relative sea-level changes in the Tasiusaq area, southern Greenland, with focus on the Ta4 basin

Daniel Fredh

Examensarbeten i Geologi vid
Lunds universitet - Kvartärgeologi, nr. 221

Geologiska institutionen
Centrum för GeoBiosfärsvetenskap
Lunds universitet
2008

Holocene relative sea-level changes in the Tasiusaq area, Southern Greenland, with focus on the Ta4 basin

Master Thesis

Daniel Fredh

Department of Geology
Lund University
2008

Contents

1 Introduction 7
1.1 Previous investigations 7
1.2 Aim 7
2 Background 7
2.1 Holocene sea-level changes 7
2.2 Southern Greenland Ice Sheet history 9
2.3 Holocene climate development 9
3 Study area 10
4 Methods 11
4.1 Fieldwork 11
4.2 Tide, threshold and GPS measurements 12
4.3 Lithological description 14
4.4 Loss on ignition (LOI) 14
4.5 XRF-scanning 14
4.6 Macrofossil analysis 15
4.7 Radiocarbon analysis 15
5 Results and interpretations 16
5.1 Tidal change and threshold elevation 16
5.2 Lithostratigraphy 17
5.3 Organic and carbonate content 18
5.4 Element variation 19
5.4.1 The supposed isolation sequence and unit 7 19
5.4.2 ”The grey layers” in units 8-10 19
5.4.3 Grey unit 11 and the supposed transgression 22
5.4.4 The complete sequence 22
5.5 Macrofossil content 22
5.5.1 Supposed isolation (unit 3 and 4) 24
5.5.2 Gyttja clay (unit 7) 24
5.5.3 ”Grey layers” (unit 9) 24
5.5.4 Grey unit 11 27
5.5.5 Supposed transgression (unit 13, 14, 15, 16 and 17) 27
5.6 Dating 28
6 Discussion 29
6.1 Basin development 29
6.1.1 Oldest sediments 29
6.1.2 Isolation 29
6.1.3 The middle part of the sedimentary sequence 29
6.1.4 Transgression 30
6.1.5 Youngest sediment 30
6.2 A sea-level curve from the Tasiusaq area 30
6.2.1 Minimum deglaciation age 31
6.2.2 The Marine Limit (LM) 31
6.2.3 The regression 33
6.2.4 The lower sea-level limit 33
6.2.5 The Neoglaciation 34
6.2.6 The transgression 34
7 Conclusions 35
8 Acknowledgements 36
9 References 36

Appendix 1. All XRF-scanned elements in the Ta4 sediment sequence.
Appendix 2a-d. Pictures of identified macrofossils.

Cover Picture: The inner Bredefjord (Nordre Sermilik) in southern Greenland. Note the small Zodiac in the centre of picture. (Photo: Dan Zwartz)

Holocene relative sea-level changes in the Tasiusaq area, southern Greenland, with focus on the Ta4 basin

DANIEL FREDH

Fredh, D., 2008: Holocene relative sea-level changes in the Tasiusaq area, southern Greenland, with focus on the Ta4 basin. *Examensarbeten i geologi vid Lunds universitet*, Nr. 221, 38 pp. 20 points.

Abstract: Until recently there have only been a few observations of relative sea-level change from the inner Bredefjord area in southern Greenland. Here a new sea-level curve is presented from the Tasiusaq area based on data mainly from a sediment sequence from a marine embayment. Sea-level changes can be recorded in sediments as changed chemical composition, physical properties and macrofossil content. Isolation and transgression sequences have been identified using lithology, loss on ignition, XRF and macrofossil analysis. Selected stratigraphical levels were AMS-dated, and additional sea level data was extracted from GPS and tidal measurements. Special attention has been given to the relation between tide and depositional environment during sea-level changes. The results suggest a rapid regression of 26 m in the Tasiusaq area between 8750 and 8050 cal. yr BP, about 1000 years later than at the coast. The sea level fell below present day level at 8050 cal. yr BP. The regression continued and the sea level reached below 3.5 m below highest astronomical tide (m b.h.a.t.) at 7300 cal. yr BP where it remained until 1210 cal. yr BP. The present day sea level was reached again sometime during the last 500 years. The marine limit was determined to c. 40 m above highest astronomical tide (m a.h.a.t.). Comparisons of the marine limit in the Bredefjord area suggest that much of the land uplift occurred before the Tasiusaq area was finally deglaciated. The transgression started also more than 2000 years later in Tasiusaq than at the coast, despite the fact that Tasiusaq is situated closer to the Greenland Ice Sheet. This anomaly can be explained by differential effects from the collapse of the Laurentide Ice Sheet peripheral bulge and the Neoglacial readvance.

Keywords: sea-level changes, isolation basin, deglaciation, Tasiusaq, Bredefjord, southern Greenland, Holocene

Supervisors: Charlotte Sparrenbom, Svante Björck, Ole Bennike and Kurt Lambeck

Daniel Fredh, Department of Geology, GeoBiosphere Science Centre, Lund University, Sölvegatan 12, SE-223 62 Lund, Sweden. E-mail: daniel.fredh@gmail.com

Havsnivåförändringar under holocen i området kring Tasiusaq, södra Grönland, med fokus på den marina lagunen Ta4

DANIEL FREDH

Fredh, D., 2008: Havsnivåförändringar under holocen i området kring Tasiusaq, södra Grönland, med fokus på den marina lagunen Ta4. *Examensarbeten i geologi vid Lunds universitet*, Nr. 221, 38 sid. 20 poäng.

Sammanfattning: Endast ett fåtal observationer har tidigare gjorts från inre delen av Bredefjorden i södra Grönland. I denna studie presenteras en ny strandförskjutningskurva från området kring Tasiusaq baserad i huvudsak på sedimentanalyser från en marin bassäng. Havsnivåförändringar registreras i sediment genom förändrad grundämneskoncentration, fysiska egenskaper och makrofossilinnehåll. Detta sker när en bassäng blir frånkopplad från havet under en regression alternativt sammankopplad med havet under en transgression. Övergångar från marina till lakustrina förhållanden (och tvärt om) i sediment har identifierats med litologi, glödförlust, XRF och makrofossilanalys, och utvalda nivåer har daterats med AMS. Dessutom har GPS använts för att mäta bassänghöjder med utgångspunkt från tidvattenmätningar vid Tasiusaq. Extra uppmärksamhet har tilldelats sambandet mellan tidvatten och depositionsmiljö i samband med havsnivåförändringarna. Resultaten tyder på att det skedde en snabb regression på 26 m i området kring Tasiusaq mellan 8750 and 8050 cal. år BP, ca 1000 år senare än vid kusten. Den relativa havsnivån föll under dagens nivå ca 8050 cal. år BP. Den relativa havsnivån fortsatte att falla till minst 3,5 m under högsta astronomiska tidvattennivån där den befann sig mellan 7300 och 1210 cal. år BP. En havsnivå motsvarande dagens nivå nåddes igen någon gång under de senaste 500 åren. Högsta kustlinjen vid Tasiusaq beräknades till ca 40 m över högsta astronomiska tidvattennivån. Jämförelser av högsta kustlinjen i Bredefjordsområdet indikerar att mycket av landhöjningen skedde innan området kring Tasiusaq var helt deglacierat. Även transgressionen skedde några tusen år senare i Tasiusaqområdet än vid kusten, trots att Tasiusaq befinner sig närmare Grönländska inlandsisen. Denna anomali kan förklaras genom att områdena påverkades olika mycket av den Neoglaciala isexpansionen och den landsänkning/landhöjning som förekom i perferin av den Nordamerikanska inlandsisen.

Nyckelord: havsnivåförändringar, isolation, deglaciation, Tasiusaq, Bredefjorden, södra Grönland, holocen

Handledare: Charlotte Sparrenbom, Svante Björck, Ole Bennike och Kurt Lambeck

Daniel Fredh, Geologiska Institutionen, Centrum för GeoBiosfärsvetenskap, Lunds Universitet, Sölvegatan 12, 223 62 Lund, Sverige. E-post: daniel.fredh@gmail.com

In the summer Eirik went to live in the land which he had discovered, and which he called Greenland, "Because," said he, "men will desire much the more to go there if the land has a good name."

- The Saga of Erik the Red -

1 Introduction

Relative sea-level changes in southern Greenland are controlled by several processes acting on both global and regional scale. The global sea level changes, on Holocene timescales, in response mainly to the redistribution of water between the ocean and the cryosphere. The Greenland Ice Sheet has varied markedly during the Holocene and possibly caused isostatic adjustments resulting in considerable relative sea-level changes in southern Greenland. Southern Greenland is also situated on the peripheral bulge zone of the ice sheets in North America and Northern Greenland, which also has an affect on the regional relative sea level. Additionally, local relative sea level could change in response to gravitation, tides, water load and meteorological changes as well as ocean temperature.

Southern Greenland is a sensitive area which is greatly influenced by changes in the ocean currents and atmospheric circulation. Studies of sea-level changes in southern Greenland can therefore be related to both glaciations and climate around Greenland and elsewhere.

During a regression/land uplift, basins situated below sea level can be lifted above sea level and end up as isolated lakes. The sediments deposited during such an isolation will change considerably. This can be seen in the lithology, chemical composition and physical properties in response to the new environmental conditions. Also the flora and fauna change in response to the transition from marine to fresh water. The opposite is true during a transgression when lakes become part of the sea. Such basins can therefore be used to study relative sea-level changes.

1.1 Previous investigations

The first observations of relative sea-level change in southern Greenland were related to the many Norse and Eskimo ruins that are partly washed away or drowned by the sea, indicating a relative sea-level rise since the time of the settlement (e.g. Mathiassen 1936). Direct measurements of the relative sea-level change from the Julianehaab and Nanortalik areas were performed by Gabel-Jørgensen and Egedal (1940) who compared observations from periods in the late 19th and early 20th century.

A few older observations of the marine limit and the regression maximum (lowest sea level) have been made in the Bredefjord area, often in connection to other type of studies. The marine limit has been indicated by lakes without any isolation (Fredskild 1973). The marine limit has also been indicated by beach ridges, raised deltas, perched boulders (Funder 1979), marine terraces (Weidick 1975), and shells found in terminal moraines (Shotton *et al.* 1974).

Some ages corresponding to a sea level at a specific time have been extracted from sediment sequences from basins that have experienced a regression (Kaplan *et al.* 2002, Funder 1979). The lowermost relative sea level is indicated by a drowned beach (Kuijpers *et al.* 1999) and by a dry crust situated below present day sea level (Bennike *et al.* 2002).

Many of the observations cited above are rather scattered and were often performed in combination with other investigations. More recent studies with focus on relative sea-level change in southern Greenland have been carried out mainly at the coast around Nanortalik and Qaqortoq (Bennike *et al.* 2002, Sparrenbom *et al.* 2006a, b). Their data consist of isolation and transgression ages, extracted from basins at different elevations. The marine limit and the lowermost relative sea level are indicated by basins without any isolation. The data have also been used for models (Bennike *et al.* 2002, Sparrenbom *et al.* 2006d). Other models from southern Greenland have been performed by Tarasov and Peltier (2002) in Julianehåb and Fleming and Lambeck (2004) from Kap Farvel.

This investigation focuses on the inner part of the Bredefjord area, where only some scattered previous observations exist. One of the basins previously studied suggests an unexpected early regression (Sparrenbom *et al.* 2006b). This early date indicates that Bredefjord could have been deglaciated early and possibly worked as a drainage path for the southern Greenland Ice Sheet. The present investigation can be seen as a continuation of previous work by Bennike *et al.* (2002) and Sparrenbom *et al.* (2006a, b).

1.2 Aim

This study focuses on sea level changes recorded in sediments from southern Greenland, and the main aim is to extract sea level data from one investigated basin. Furthermore, these data are put together with data from a parallel study by Randsalu (2008) to construct a new sea-level curve. Another aim is to evaluate some relations to glaciation and climate, but also the importance of the Bredefjord area as a drainage path for the Greenland Ice Sheet.

2 Background

2.1 Holocene sea-level changes

Since the minimum position in global sea level, about 130 m below present at the Last Glacial Maximum (LGM), the global sea level experienced a nearly uniform rise between 15 000 to 7000 cal. yr BP (Fleming *et al.* 1998). During the last 7000 years the global sea level has been almost constant, apart from a probable rise of 3 to 5 m completed at 2000 to 1000 cal. yr BP, without any significant oscillations (Fleming *et al.* 1998).

The first sea-level curve from the outer coast of southern Greenland was constructed by Bennike *et al.* (2002). The marine limit in the Nanortalik region is set between *c.* 32 and 46 m above highest astronomical

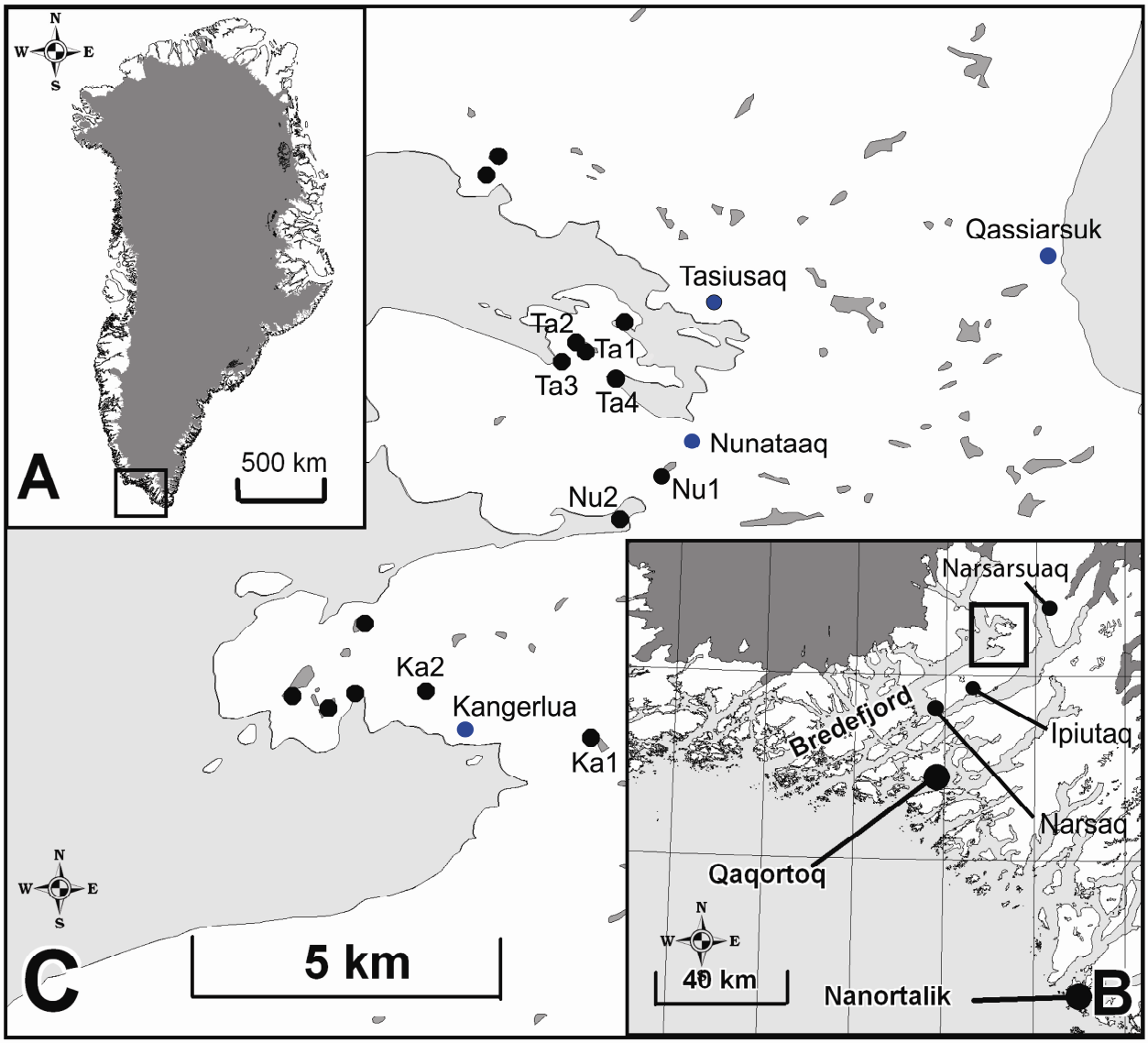

Figure 1. A: Map of Greenland where the rectangle marks the Julianehåb district. B: Map of the Julianehåb district in southern Greenland with a rectangle that define the main study area. C: Map showing the study area with investigated basins (black dots). Blue dots represent villages or farms.

tide (m a.h.a.t.), which corresponds to a level between lakes with and without isolation (Bennike *et al.* 2002). Investigated isolation basins in the Nanortalik area suggest a rapid relative sea level fall between 11900 to 10200 cal. yr BP, and that the relative sea level was below present day level during most of the Holocene (Bennike *et al.* 2002).

Sparrenbom *et al.* (2006a) extended this sea level curve with data from basins below present sea level, which made it possible to study also the relative sea level changes during the latest 10000 years. The relative sea level fell below present sea level at around 9300 cal. yr BP and continued to fall until at least 9000 cal. yr BP (Sparrenbom *et al.* 2006a). The lowermost basin studied with an isolation (and transgression) is situated at *c.* 7.8 m below highest astronomical tide (b.h.a.t.) and constitutes a minimum level of the local regression. Sparrenbom *et al.* (2006 a) concluded that the lowermost sea level during the Holocene must have been about 10 m b.h.a.t. between *c.* 8000 and 6000 cal. yr BP. A gradual transgression with a mean rate of 1.5 to 2 mm per year, started before 5000 cal. yr BP. This transgression was caused by a readvance of the southern Greenland Ice Sheet and/or a delayed collapse of the peripheral bulge of the Laurentide Ice Sheet (Sparrenbom *et al.* 2006a).

In the Qaqortoq area the pattern is similar; the relative sea level was situated at *c.* 31.0 m above highest astronomical tide (a.h.a.t) at *c.* 11 000 cal. yr BP and fell rapidly and reached below 2.7 m b.h.a.t. at 8800 cal. yr BP (Sparrenbom *et al.* 2006b). However, this happened later than in Nanortalik, which is explained by different distances to the coast. The marine limit is indicated to be above a lake with an isolation sequence at 31 m a.h.a.t. and below perched boulder found at 52 to 54 m a.h.a.t. (Sparrenbom *et al.*

2006b). The minimum relative sea level in Qaqortoq reached below an isolated basin at 2.7 m b.h.a.t and above a marine basin without any lake sediment at 8.7 m b.h.a.t., corresponding to an age between 8000 and 4000 cal. yr BP (Sparrenbom 2006b). The transgression started at the latest at 4000 cal. yr BP with a mean relative submergence of *c.* 3 mm per year (Sparrenbom *et al.* 2006b).

Further inland Funder (1979) estimated the marine limit to be slightly higher in the Narsaq area: between 33 and 59 m a.h.a.t. Even further inland at Ipiutaq a lake at 39.7 m a.h.a.t. have been investigated, but without any isolation found, suggesting that the marine limit in this area is lower than 40 m a.h.a.t. (Sparrenbom *et al.* 2006b). However, perched boulders are found close to Ipiutaq at 40 to 45 m a.h.a.t. (Sparrenbom *et al.* 2006b). A dry crust was found outside Narsaq at *c.* 10 m b.h.a.t. (Bennike *et al.* 2002), which indicates the minimum relative sea level there.

Previuos observations of relative sea-level changes from the area around the inner Bredefjord are more scattered. Fredskild (1973) observed an upper limit (a lake without isolation) of relative sea level at *c.* 64 m a.h.a.t. close to Qassiarsuk. Fredskild (1973) also observed beach ridges at 36 m and Weidick (1975) found a marine terrace at 10 to 20 m a.h.a.t. at Narsarsuaq. Their observations suggest a marine limit between 36 and 64 m a.h.a.t.

The only indicator of a low sea level found in the inner parts of the fjords is a drowned beach *c.* 110 metres outside Qassiarsuk, at *c.* 4 to 5 m b.h.a.t. (Kuijpers *et al.* 1999). The only basin with an isolation sequence investigated from the inner Bredefjord is a lake (Nu1) situated at Nunataaq, at *c.* 9.6 m a.h.a.t. with an isolation dated to *c.* 11 250 cal. yr BP (Sparrenbom *et al.* 2006b). The date is the oldest obtained from the whole Bredefjord area, which indicates an early deglaciation of the ice sheet: the Bredefjord could have acted as a calving bay, with a rapidly disintegrating floating glacier (Sparrenbom *et al.* 2006b). However, the relative sea-level change in the inner part of the ice free land areas is still uncertain.

2.2 Southern Greenland Ice Sheet history

The ice sheet in southern Greenland was substantially larger during the LGM than today, probably reaching out to the shelf margin (Bennike *et al.* 2002, Bennike and Björck 2002, Weidick *et al.* 2004, Sparrenbom *et al.* 2006d). The ice thickness in the Nanortalik region at the outer coast during LGM must have been more than 1500 m (Bennike *et al.* 2002) and in central southern Greenland in the order of 4300 m (Sparrenbom *et al.* 2006d). A rapid melting of the Greenland Ice Sheet during the Late glacial and early Holocene is indicated by the rapid fall in relative sea level observed in the Nanortalik and Qaqortoq regions during early Holocene (Bennike *et al.* 2002, Sparrenbom *et al.* 2006b). Late glacial lake sediments have also been found at the outermost coast (Bennike and Björck 2002), indicating that the ice sheet retreated onto the present coast before the onset of the Holocene. Possibly the retreat was interrupted by the Neria stade, a shorter readvance of Younger Dryas age (Weidick *et al.* 2004).

Lake sediments from the inner Bredefjord have been dated to *c.* 9500 cal. yr BP at Qassiarsuk (Fredskild (1973) and to *c.* 11 250 cal. yr BP at Nunataq (Sparrenbom *et al.* 2006b), which indicate that the inner fjord areas was deglaciated before this time. Models by Sparrenbom *et al.* (2006d) indicate that the ice sheet reached its present day position at *c.* 10 500 cal. yr BP and a minimum ice sheet 30 km behind present day margin at *c.* 9000 cal. yr BP. One local readvance at about 8000 to 7000 cal. yr BP are recorded by the Tunugdliarfik moraine system (Weidick *et al.* 2004). That the ice sheet has been smaller than present is shown by reworked non-glacial material in the neoglacial moraines (Kelly 1980).

Kelly (1975) dated a maximum age of the neoglacial readvance to *c.* 5300 cal. yr BP from a site in the outer part of Bredefjord. Weidick *et al.* (2004) concluded that the neoglacial readvance may have begun at 3000 to 4000 cal. yr BP. Modelling by Sparrenbom *et al.* (2006d) suggests a start of the neoglacial advance before 6500 cal. yr BP with the ice sheet reaching the present day margin at *c.* 5500 cal. yr BP.

Erratics in the Narsaq area indicate a minimum thickness of the ice cover to be 1200 m (Funder 1979). The high amount of erosion in the Julianehåb district indicates a warm based ice, at least during some part of the glaciation (Weidick 1987).

The maximum neoglacial extent of most glaciers was reached between 100 to 200 years ago (Weidick 1984, Weidick *et al.* 2004, Bennike and Sparrenbom 2007). One exception is the Narsarsuaq stade that has been dated by sediments between end moraines to older than about 1200 cal. yr BP where the end moraines are suggested to have formed about 2000 years ago (Bennike & Sparrenbom 2007).

2.3 Holocene climate development

The Holocene climate in southern Greenland has been studied from lake sediments (Fredskild 1973, Kaplan *et al.* 2002, Ljung & Björck 2004, Andresen *et al.* 2004) and from measurement from the GRIP and Dye 3 ice bore holes (Dahl-Jensen 1998).

According to Dahl-Jensen (1998) the temperature at the ice sheet summit during LGM was about 23 degrees K colder than today. The transition from the Late glacial to the Holocene in southernmost Greenland was characterized by a change from dry and cold climate to a more humid and mild climate (Andresen *et al.* 2004). However, during the earliest Holocene, short scale fluctuations are recorded, before a more stable climate was reached at 9300 cal. yr BP

(Andresen *et al.* 2004). Results from Ljung & Björck (2004) suggest that the extensive sea ice cover started to break up in the beginning of the Holocene, but the interglacial mode in the fjords was delayed due to the many icebergs calving from the receding ice sheet.

The Holocene climate optimum occurred between 8000 and 5000 cal. yr BP, suggested by high precipitation during that period (Andresen *et al.* 2004). The same period for the climatic optimum is suggested by Dahl-Jensen (1998) and calculated to be 2.3 degrees K higher than present. However, Kaplan *et al.* (2002) date the Holocene thermal maximum in southern Greenland to have occurred between 6000 and 3000 cal. yr BP.

Andresen *et al.* (2004) have recorded a distinct change to colder and drier conditions from 3700 cal. yr BP, but interpret the initiation into colder climate to have started at *c.* 4700 cal. yr BP. Kaplan *et al.* (2002) record a marked cooling shortly after 3000 cal. yr BP, followed by more unstable climatic conditions which culminated during the Little Ice Age (LIA). The last part of the LIA is also recorded as the most severe interval during the entire Holocene period (Kaplan *et al.* 2002). Exceptions are two reversals at 1300 to 900 cal. yr BP and 500 to 280 cal. yr BP, corresponding to Medieval Warm Period (MWP) and a warmer period prior to the second part of the LIA respectively (Kaplan *et al.* 2002). Instead, Andresen *et al.* (2004) point out two drier periods at 3700-2400 cal. yr BP and 1800-600 cal. yr BP.

The climate change in southern Greenland is explained by Andresen *et al.* (2004) as a result of the different positions of the Icelandic low pressure. When the Icelandic low pressure is close to Iceland and southern Greenland the climate in southern Greenland is characterized by relatively high temperatures and increased precipitation. A position of the low pressure closer to Barents sea is accompanied with an extension of the high pressure cell over Greenland, which led to a more dry and cold climate with an increase in storminess in our study area (Andresen *et al.* 2004).

The only climatic indicators from the inner parts of the fjords are extracted from vegetation studies close to Qassiarsuk (Fredskild 1973). The vegetation suggests that climatic conditions between *c.* 9700 and 9000 cal. yr BP correspond to the area at the west coast today, between 67° and 69° N. The climatic contitions between *c.* 7700 and 5200 cal. yr BP are interpreted as favorable, not much different from today (Fredskild 1973). The vegetation also suggests drier and warmer conditions between *c.* 5200 and 3900 cal. yr BP and indicates wetter conditions after *c.* 3900 cal. yr BP (Fredskild 1973). Again lower preciptation betweeen *c.* 1900 and 900 cal. yr BP has been recorded (Fredskild 1973).

3 Study area

The main study area is situated in the inner Bredefjord (Nordre Sermilik), close to Tasiusaq village (Fig. 1). Bredefjord constitutes a part of the Julianehåb district (N60-61.5°, W45-47°), where the towns Nanortalik, Quaqortoq and Narsaq are situated, in former times known as the Norse eastern settlement. Bredefjord is about 600 m deep and around 75 km long and one of several parallel fjords in the region, formed in a general ENE-WSW direction.

The fjord is flanked on both sides by bedrock, composed of granite, sandstone and lavas. The topography is controlled by the different bedrocks resistance to glacial erosion and weathering (Funder 1979). In a regional context the bedrock in southern Greenland is dominated by a 1.8-2.0 Ga old granite formed in a subduction zone, the Julianehåb batholith (Sørensen 2006). Between Narsarsuaq and Narsaq, flanking the Bredefjord, known as the Gardar province, sandstone and lavas were formed at 1.3 Ga ago by intrusions in a rifting setting (Sørensen 2006). The bedrock at the highest altitudes at 1500 metres is composed of sandstone and lavas, whereas the Julianehåb granite rarely reaches 500 metres (Funder 1979). The sandstone has been cemented by iron oxide, which gives the sandstone a reddish colour (Sørensen 2006).

The climate in southern Greenland is low-arctic and influenced by its proximity to the ocean. The outer part of the fjords in southern Greenland is closely linked to the variability of the North Atlantic open-ocean circulation (Lassen *et al.* 2004, Jensen *et al.* 2004). The inner parts of the fjords are more influenced by the effect of local air temperature, melt water run-off and wind conditions (Jensen *et al.* 2004). Two surface ocean currents influence the climate in southern Greenland. First, the East Greenland Current (EGC) characterised by cold, low salinity, polar waters that flow southwards along the east coast, which carries icebergs and pack ice from the Arctic Ocean and from the fjords in east Greenland (Andresen *et al.* 2004). Second, the Irminger current that moves southwestwards containing warm and saline Atlantic water (Andresen *et al.* 2004). Both currents meet outside the southeast coast of Greenland, mixes and continue up the west coast of Greenland where the ice melts (Andresen *et al.* 2004).

The climate in Greenland is also affected by the North Atlantic Oscillation (NAO), which controls the strength and direction of westerly winds and storm tracks across the North Atlantic. During the winter low pressure system crosses south Greenland from southwest to northeast, making the weather change between clear and cold weather with north westerly winds and eastern winds with higher temperatures and increased precipitation (Andresen *et al.* 2004).

Temperature and precipitation in southern Greenland differ naturally with distance to the coast. From the inner parts of Tuniarlifik fjord in Narsarsuaq,

Figure 2. The marine embayment Ta4, situated close to Tasiusaq, inner Bredefjord. The main study site from where a sediment sequence was investigated. (Photo: Charlotte Sparrenbom)

the temperature has been measured during the warmest month in July to 10.3°C and in the coldest month January to -6.8°C, with an annual precipitation of 616 mm (Cappelen *et al.* 2001). In Qaqortoq at the outer coast the temperature ranges between 7.2 in July to -5.5 in January, with a precipitation of 858 mm per year (Cappelen *et al.* 2001).

Several outlet glaciers from the inland releases large amounts of icebergs into the Bredefjord and in higher areas local ice caps occur. The study area is surrounded by inland ice in three directions with 25 to 50 km to the ice sheet in the west, north and east. The ice cap in the east is called the Julianehåb ice cap and has the character of a regional ice sheet, only loosely connected to the Greenland Ice Sheet in the north. The Bredefjord area has been subject to substantial erosion, with only few Quaternary deposits remaining (Weidick 1987).

The vegetation in the study area is dominated by Salix glauca, but common are also Betula pubencens and B. glandulosa that cover large areas (Fredskild 1973). In the area also Kobresia and grass heaths are found (Fredskild 1973).

The area close to the Tasiusaq village is situated in a protected embayment with the marine basin (Ta4) investigated in this study. The basin is situated next to a peninsula, surrounded by reddish sandstone and the Julianehåb granite. The marine basin has an elongated shape with a size of about 180 x 90 metres (Fig. 2). The slopes surrounding the basin are gentle and reach about 50 m a.h.a.t., at several places covered by raised beaches. There is no fresh water stream into the basin, suggesting that fresh water supply to the basin is restricted to ground water and/or by surface runoff.

4 Methods

4.1 Fieldwork

Fieldwork was carried out in August and September 2007. Sediments with potential isolation and transgression sequences from totally 11 lakes and 3 marine embayments were collected from basins around Tasiusaq, Nunataq and Kangerlua in the inner part of Bredefjord. The basins are situated within an area of about 8 x 8 km, and are therefore probably affected by a similar rebound and/or subduction during the Holocene and can be used for the reconstruction of Holocene sea level changes. The lakes and marine basins have no names and different codes are therefore

Figure 3. Coring of the marine embayment Ta4 from a Zodiac dinghy with a Russian corer (Dan Zwartz, Daniel Fredh and Linda Randsalu). (Photo: Charlotte Sparrenbom)

used, depending on there proximity to named farms or villages (Ta1, Ta2, Nu2 etc.)

One marine embayment (Ta4) was selected as the main study site for this investigation. The bathymetry of the basin was measured by an echo sounder to find the most suitable coring site. Coordinates of the coring position was measured with a handheld GPS to N 61°08,050', W 45°39,200'. The coring took place from a Zodiac dinghy with a platform attached with ropes at the shoreline (Fig. 3). The water depth during coring varied between 2.7 and 4.2 m depending on the tide level. The coring site was selected to the deepest part, approximately in the middle of the basin. Sediment between 2.70 m and 9.93 m below sea level was collected in overlapping sequences with a Russian corer with a length of 1 m and a diameter of 5 cm. The cores were described briefly in field before they were wrapped with plastic and put in plastic half tubes, before they were shipped to Lund and stored at 4°C.

4.2 Tide, threshold and GPS measurements

To be able to more accurately work out the relative sea-level change in an area with significant tidal effects it is necessary to collect data about the local tide. The closest prediction of the tidal change is from Narsaq about 25 km from the study area. The tidal change in Narsaq is 3.4 metres between the lowest (neap) and highest (spring) tides (Farvandsvæsenet 2006). The tide depends on astronomical and meteorological variations, here assumed to be similar during the Holocene. The tide fluctuates about twice a day but only rarely reach maximum and minimum levels. The spring tide that corresponds to approximately the highest predicted value in Narsaq is reached twice a month when the moon and the sun are aligned. The meteorological contribution adds to this tidal range. The highest possible tide from both the astronomical and meteorological contributions constitutes the highest astronomical tide (h.a.t.), which

are used as a reference level in this study. Additionally, storm events could occasionally raise the sea level even further, but are here assumed not to influence the basin markedly. The tide change locally due to bathymetry, passages etc. Therefore, the predictions in Narsaq could differ both in time and height from the study area.

To be able to more accurately calculate the highest astronomical tide in the study area a tide gauge was used to measure the sea-level variation (Fig. 4). The tide gauge was lowered into the sea at about 7 m depth close to the Tasiusaq village and remained in place for about 5 days. The tide gauge measured the pressure that depends on the water load, i.e the water depth.

The threshold (sill) of a lake is the lowest level that surrounds a basin, where the water usually flows out. In a marine basin the water flows over the threshold in both directions twice a day due to the tidal currents. The threshold elevation determines if and when a basin is connected to the sea, which is of greatest interest when studying sea-level change through time. Due to the local tidal change a basin can be connected to the sea the whole or parts of a day. If the relative sea-level change occurs rapidly, the interval when a basin is only partly connected to the sea (within the tidal span) is often recorded within a few centimetres distinct layering (also depending on the sedimentation rate). However, if an isolation or transgression happens more slowly, the recorded transition in the sediment is gradual and can cover a longer sequence. The marine basin (Ta4) investigated in this study possibly have a relatively high sedimentation rate and both slow isolation and transgression sequence. Therefore, the different conditions during these transitions are here investigated in more detail.

The conditions in these basins can vary between lacustrine, marine or brackish, but it is not totally clear when these condition occur in relation to a certain sea level. It is, however, reasonably to assume that when only the highest tides reach into a basin, the basin environment is still dominated by lacustrine conditions. The opposite is true when a basin is cut of from the sea only during the lowest tides; then the basin is still dominated by marine conditions. A basin is thought to be totally isolated when the sea level cease to reach into the basin during the highest astronomical tide. The first sign of transgression is thought to occur when the sea water just starts to enter the basin at highest astronomical tide.

During a regression a basin with a threshold level just above neap tide level will be cut off from the sea partially and totally isolated first when the highest tide becomes lower than the threshold level and therefore marine water ceases to enter the basin. During a transgression, a brackish phase will start sometime after the first incursion, i.e. when the highest astronomical tide first enters the basin and the basin will become more and more marine influenced as the sea can flow into the basin longer and longer periods during the day. The brackish phase could crudely be described to correspond to the tidal span and is possibly recorded in the sediments. By dating the first and/or last marine influence in a basin as well as the change into a fully marine or fully lacustrine environment, we could theoretically date relative sea-level changes twice in the same basin because of the

Figure 4. A tide gauge attached to a metal piece ("anchor") was used to measure the tidal range outside Tasiusaq (left). (Photo: Charlotte Sparrenbom) The portable unit in the GPS-equipment was used to measure the height of e.g. the sea-level and basin thresholds in the study area (right). (Photo: author)

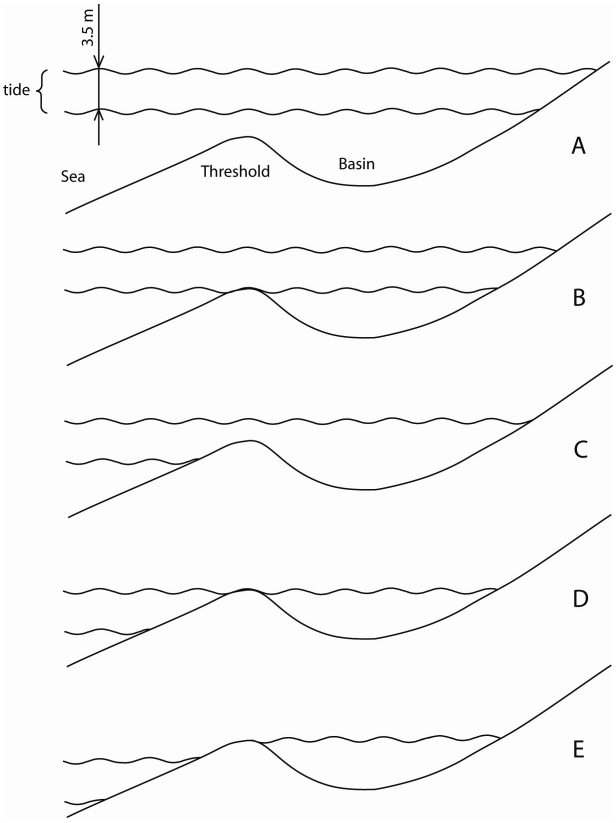

Figure 5. Principal sketch of different environmental conditions in a basin at different relative sea-levels. A: Totally marine conditions. B: At the limit between marine and brackish conditions. C. More or less brackish conditions. D: At the limit between lacustrine and brackish conditions. E: Totally lacustrine conditions. The limits in B and D are possibly recorded in the basin sediment.

tidal span. This theory is displayed in Figure 5. In practice it can be very tricky to accomplish this as erosion and resedimentation is common in these basins, which are strongly affected by tidal currents going in and out twice a day.

The threshold of Ta4, the marine basin investigated in this study, was measured with a rod from the Zodiac dinghy during a specific time. By combining this measurement from the tide gauge and the Narsaq predictions combined with an estimation of the climate contributing factor, the threshold elevation related to the highest astronomical tide can be calculated. To connect the tidal measurement to other sea-level indicators, e.g. lake elevations and beach ridges, the sea level was also measured with GPS.

The GPS equipment used was a base station that remained stationary for about 6 days, at the same time as a portable unit was used to measure different heights and positions at all the sites visited (Fig. 4). Each measurement lasted *c.* 20 minutes. The accuracy for the GPS measurement lies within a few centimetres in altitude (Dan Zwartz, personal communication).

The threshold measurement is accompanied with some uncertainties. The total uncertainty can be calculated with the formula $\sigma_{total} = (\sigma_1^2 + \sigma_2^2 + \sigma_3^2)^{1/2}$ (Sparrenbom *et al.* 2006a), where σ_1^2 is the uncertainty of threshold measurement, σ_2^2 the uncertainty of threshold development and σ_3^2 the uncertainty of the tidal measurement.

4.3 Lithological description

The cores were correlated visually in the laboratory. The cores were also photographed and described with respect to lithology, colour and boundary characteristics.

4.4 Loss on ignition (LOI)

The loss on ignition method can be used to calculate the organic and carbonate composition in sediment samples. The method is based on weighing the samples before and after heating at different temperatures (Dean 1974). The Ta4 sediment sequence was subsampled every 10-15 cm and more closely spaced where lithological changes occur. These samples were treated as follows (Heiri *et al.* 2001): samples were dried at 105°C for 12 to 24 hours. Then the samples were heated in a furnace in two steps at 550°C for 4 hours and 950°C for 2 hours. In the first step the organic material is combusted into carbon dioxide and ash and in the second step the carbon dioxide is evolved from carbonate minerals. Between each step the samples are cooled in a desiccator before weighing. Organic and carbonate content was calculated from formulas in Heiri *et al.* (2001) as percent of dry weight.

4.5 XRF-scanning

X-ray fluorescence spectrometry (XRF) method measures the relative amount of a choice of elements in a sediment sequence. The elements in a sediment sequence are thought to vary in response to climate and/or depositional environment (Sparrenbom *et al.* 2006c). XRF-scanning have been used both in climatic studies (Daryin *et al.* 2005), and in sea-level studies to identify isolation/transgression levels (Sparrenbom *et al.* 2006b). To aid the identification of the levels of isolation and transgression in the Ta4 sediment sequence, a choice of elements were measured with XRF in intervals selected by the lithologically described changes.

In several sediment sequences, K, Ca, Ti, Mn, Fe, Co and Sr have previously shown strong decline at the isolation contact whereas Cu increases (Sparrenbom *et al.* 2006b). According to Sparrenbom *et al.* (2006c) the composition of the sediments and variations within are roughly controlled or indirect controlled by redox conditions (Fe, Mn, S, Ba, Zn and Cr), available minerals (Al, Si, K, Rb, Ti, Zr, P, Ca and Sr) or the production of organic matter and elements bound to organic matter (Se, Cu, Ni and Pb). The Si/Ti ratio can be used as a proxy for biogenic

Table 1. Lithostratigraphy of the marine embayment (Ta4) sediement sequence

Unit #	Depth (cm)	Description
16	400-446	Dark grey, silty, sandy clay gyttja. Gravel occur sporadic. Shell accumulation at 427-431. Vague sand layer at 445-446.
15	446-459	Gradual transition from black silty, clayey, sandy coarse detritus gyttja to dark grey, sandy, clay gyttja. UB: Gradual
14	459-502	Black, silty, clayey, sandy coarse detritus gyttja. Even coarser detritus at 479-484 and 492-495. UB: Gradual
13	502-519.5	Light brown to black, laminated, clayey fine detritus gyttja. Coarse detritus at 510-512 and 514-515. UB: Gradual
12	519.5-561.5	Light brown, dark brown and red brown layers (0.1-5.0 cm thick) of clayey, silty fine detritus gyttja. UB: Sharp
11	561.5-570.5	Dark grey, clayey, sandy, silt gyttja. UB: Rather gradual
10	570.5-651.5	Light brown, dark brown and red brown layers (0.1-6.0 cm thick) of clayey, silty, fine detritus gyttja. UB: Sharp
9	651.5-662	Dark grey, light brown and dark brown layers. Three dark grey layers (0.3-0.7 cm thick) of sandy, clayey silt gyttja. Five dark brown layers (1.0-2.0 cm thick) and two light brown layers (1.5 cm thick) of clayey fine detritus gyttja to clay gyttja. UB: Rather gradual
8	662-887.5	Light brown, dark brown and red brown layers (0.1-10 cm thick of clayey, silty fine detritus gyttja. UB: Rather sharp
7	887.5-888	Light grey gyttja clay. UB: sharp
6	888-898.5	Light brown to dark brown layers (0.5-3.0 cm thick) of clayey, silty fine detritus gyttja. UB: Sharp
5	898.5-911.5	Light brown to brown, clayey, silty fine detritus gyttja. UB: Sharp
4	911.5-913.6	Dark brown, silty clay gyttja. UB: rather gradual
3	913.6-918.2	Laminated silt gyttja (with grey, light brown and dark brown lamina). UB: Sharp
2	918.2-954	Grey, silty gyttja clay to grey silty clay gyttja. UB: Sharp
1	954-991	Grey, silty sandy clay. UB: Gradual

UB = Upper boundary

silica production (Moreno *et al.* 2007). Common elements in marine sediment are Ca, Fe, Sr, K and Ti (Böning *et al.* 2007).

The scanning was carried out on an Itrax XRF Core Scanner at Stockholm University. Before the cores were scanned each core was cleaned and covered by a thin plastic film. The selected intervals were scanned in steps of 2 mm measuring 20 seconds at every step. The data has then been recalculated to counts per second.

4.6 Macrofossil analysis

Macrofossil analyses were carried out in the Ta4 sediments to identify the depositional environment. Many animals and plants are restricted to salt, brackish or fresh water, and indicate if a basin was connected to the sea or was a lake during the time of deposition. Macrofossil analysis of a sediment sequence is therefore an important tool to pinpoint the stratigraphic level where an isolation or a transgression might have occurred.

The sediment sequence was subsampled at different intervals depending on the lithological changes. More closely spaced sampling was done around lithological boundaries. The volume of the samples were measured before they were wet-sieved using a 0.2 mm sieve. Identification of the different macrofossils and what they indicate have been aided by Foersom *et al.* (1997), Rueness (1977), Böcher (2001) and Nilsson (1961), but also directly by Ole Bennike and Charlotte Sparrenbom. The identification was done in a stereo microscope and the identified macrofossils also provided material for ^{14}C dating.

4.7 Radiocarbon analysis

To be able to establish the age of isolation and transgression of the Ta4 basin, AMS-radiocarbon dating was carried out on several macrofossil samples from the identified environmental changes registered in the sediment sequence. The dated material consisted of terrestrial macrofossils and bulk sediments. The dating was carried out in the Radiocarbon Dating

Laboratory in Lund and calibrated using the software OxCal v.3.10, based on the terrestrial data from Reimer *et al.* (2004) and the marine data from Hughen *et al.* (2004).

5 Results and interpretations

5.1 Tidal change and threshold elevation

The measured tidal change close to Tasiusaq is shown in Figure 6. The water depth during the measurement varied between 5.8 and 7.6 m, corresponding to a tidal span during this period of 1.8 m. The tidal measurements at Tasiusaq coincide with a period of low tides. The tidal predictions in Narsaq by Farvandsvæsenet (2006) are given every 6 hours, and a comparison between the predictions and the observations for the measured period is also shown in Figure 6. The comparison shows that neap tide in Narsaq corresponds to 5.1 m of water depth at the observation site at Tasiusaq.

The observations in Tasiusaq deviate somewhat in both time and tidal range from the predictions in Narsaq, which suggests that there are some discrepancies between the two areas. The tidal range differs about 0.1 to 0.2 m during the period of measurement. However, the measured period is thought to be too short to exact determine the tidal difference, and therefore the spring tide predicted in Narsaq at 3.4 m are interpreted to be similar in the Tasiusaq area. When adding 0.1 m for the meteorological contribution (approximately the value used at Qaqortoq (Sparrenbom *et al.* 2006b)), the tidal range is set to 3.5 m between lowest astronomical tide (LAT) and highest astronomical tide.

The basin threshold was measured with a coring rod from a Zodiac dinghy to 1.0 m below water level at 5.45 p.m. local time, 19.45 Universal Time Corrected (UTC) the 18th August. The tide gauge measurement show a water depth of 6.1 m at the observation site at this time. By adding what is left to the highest astronomical tide (in the Narsaq tidal range) with the water depth, the threshold elevation is calculated to 3.5 m b.h.a.t.

The threshold is, according to this calculation, situated at an elevation where the basin is exactly at the limit between being connected to and cut off from the sea during the lowest tides. The threshold is composed of bedrock and boulders, and we therefore assume that the threshold elevation has not changed much through time.

The low and high tide was also measured with GPS in the study area and compared to the tidal measurements (Table 2). All measured GPS heights in Tasiusaq are tied to the G701 high tide measurement.

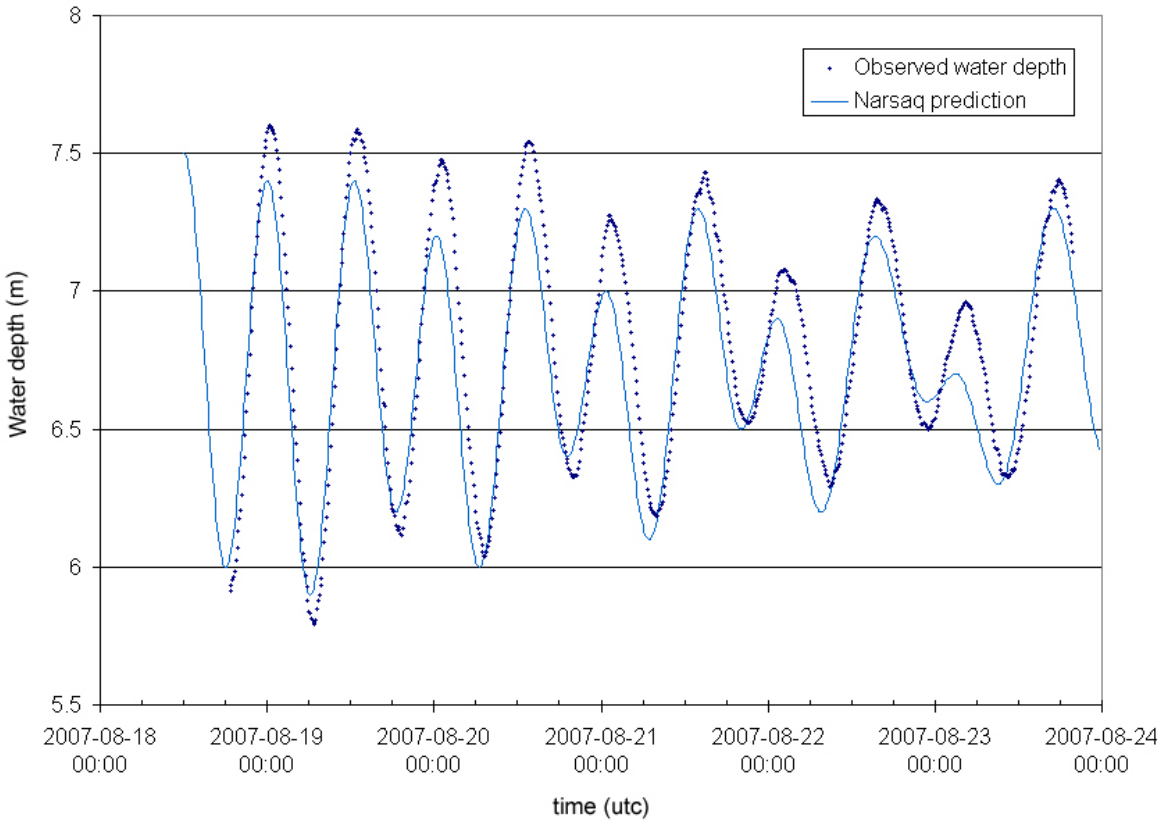

Figure 6. Tidal measurements at Tasiusaq compared to tidal predictions in Narsaq. The tidal measurements are used to calculate the highest astronomical tide, which are used as reference level for all height measurements in this study.

Table 2. GPS measured sea level indicators in the study area

GPS no.	Lat	Long	Type of measurement	Measured hight m a.h.a.t.
G701	61.13621	314.3567	High tide at Tasiusaq 19.8.07 10h49, value set from tide gauge and tables	-1.0
G709	61.13415	314.3457	Low tide at Tasiusaq 19.8.07 17h00, expected to be -2.7 according to tide gauge	-2.67
G702	61.1362	314.3566	Focus line, highest main band of stranded sea weed	-0.24

A total uncertainty estimate is done and the result is shown in Table 6. The uncertainty of the measurement with the rod is estimated to 0.1 m. For the interpretation of the exact threshold position and the threshold development through time, an uncertainty estimate of 0.3 m is assumed. The tidal uncertainty is set to 0.5 m due to the uncertainty in tidal development through time and fjord effects compared to the Narsaq predictions.

5.2 Lithostratigraphy

The nine visually correlated cores constitute a total sediment sequence of 5.91 m. The sequence was divided into 16 units depending on their different lithology (Table 1). All the depths are related to cm below water level.

Unit 1 and 2 in the bottom of the sequence is composed of grey, silty clay to clay gyttja with slowly increasing amount of organic matter and decreasing sand content. Unit 3 and 4 constitute a transition from previous units into fine detritus gyttja in unit 5 with gradually increasing organic content. Unit 3 is a laminated silt gyttja with grey and brown lamina, and differ from unit 4, which is more homogeneous and has a darker brown colour. Unit 3 and 4 are though to represent an isolation sequence that is investigated in more detail with XRF and macrofossil content (Fig. 7A).

The units 5, 6, 8, 10 and 12 are very similar; fine detritus gyttja, with varying colours constitute the dominant type of sediments in these units. The first impression of these units is that they are of lacustrine origin. The reddish colour in parts of these units can be explained by the iron rich bedrock surrounding the basin.

The fine detritus gyttja in the middle part of the sequence is interrupted in three places by grey, more minerogenic sediments (unit 7, 9 and 11). Unit 7 is 0.5 cm thick and rich in clay, probably deposited during one short event (Fig. 7B). Unit 9 is composed of several thin recurrent grey layers, covering 10.5 cm (Fig. 7C). Unit 11 is a distinct silt gyttja, 9 cm thick,

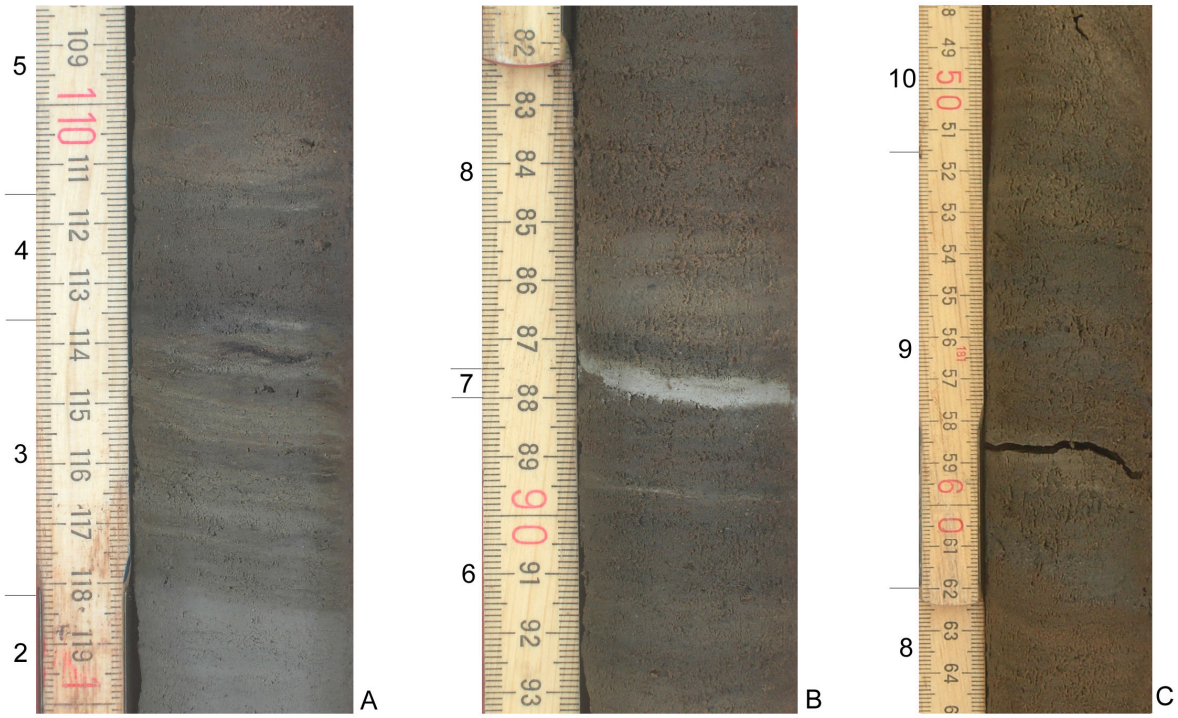

Figure 7. Pictures of selected intervals from the Ta4 sediment sequence. A: Supposed isolation sequence (units 3 and 4). B: Gyttja clay (unit 7). C: Grey layers in unit 9. Unit numbers are displayed at the left side. (Photos: Author)

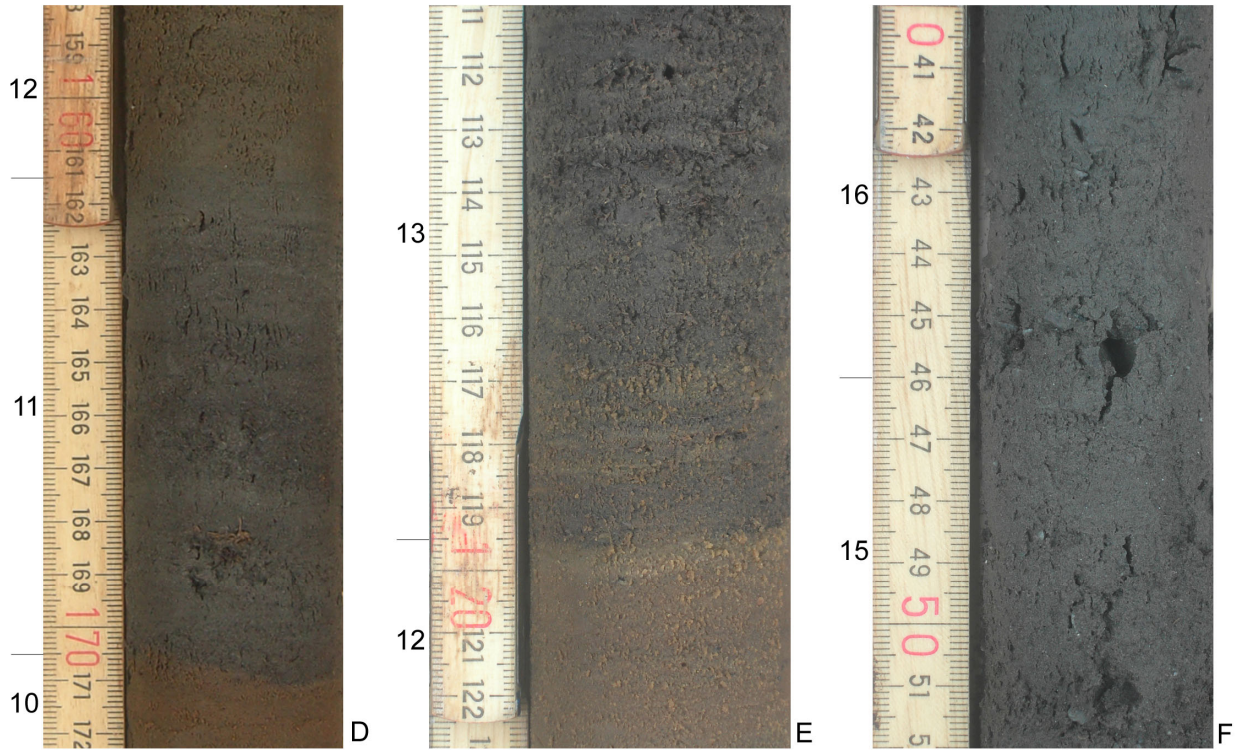

Figure 8. Pictures of selected intervals from the Ta4 sediment sequence. D: Silt gyttja (unit 11). E: Supposed first sign of marine influence in the transgression sequence (unit 13). F: Boundary between units 15 and 16. Unit numbers are displayed at the left side. (Photos: Author)

and could have been deposited as either one event or during a somewhat longer time (Fig. 8D). From their appearance it is not clear if these units have a marine origin, if the sea level was at or close to the threshold of the basin or if they are lacustrine. Therefore, these units were investigated further with XRF and macrofossil.

Unit 13, 14 and 15 constitute a transition from fine detritus gyttja (unit 12) to grey clay gyttja (unit 16) with a general increase in minerogenic content (Fig. 8E, F). The transition contains coarse detritus and increased amounts of sand, mainly in unit 14. Gravel and shell accumulation occur in the uppermost unit 16, with an otherwise similar appearance as unit 1 and 2 in the lowermost part of the sequence. Unit 13, 14 and 15 are thought to represent a transgression sequence during a sea-level rise and are investigated in more detail with XRF and macrofossil.

5.3 Organic and carbonate content

The organic and carbonate content was measured with LOI in almost the entire sediment sequence, in different steps between 954 to 425 cm depth (Fig. 9). The sampled intervals varied between 0.5 and 15 cm; a denser sampling was carried out around lithological boundaries. The organic content varies between 3.4% and 53% and the carbonate content varies between 0 and 6.1% (Fig. 9).

The organic content in unit 1 and 2 in the bottom of the sequence varies between 5.7 and 8.6%. Unit 3, 4 and the beginning of unit 5 show a rapid increase of the organic content from 12 to 28%. The organic content in unit 5, 6, 8, 10, 12 varies between 17 and 40%. The thin unit 7 has only one measurement of organic content (4.6%). The organic content in unit 9 shows a high variability, between 7.6 and 29%, as could be expected from the variability in the lithology. Unit 11 deviates from surrounding units with lower values, 6.2 to 8.5%. In unit 13 the organic content increases from 37 to 53%. From the lower part of unit 14, up to the top part of unit 16, there is a decreasing trend in organic content with a few deviting peaks, showing values between 3.4 up to 41%. The units with most minerogenic content are units 1, 2, 7, 9, 11, 15 and 16. The unit with most organic content is unit 13.

The carbonate content is generally low with less accuracy as a consequence. The carbonate content shows a similar curve as the organic matter and changes at lithologic boundaries. However, the carbonate content does not show any clear difference between the minerogenic or organic rich units as a whole.

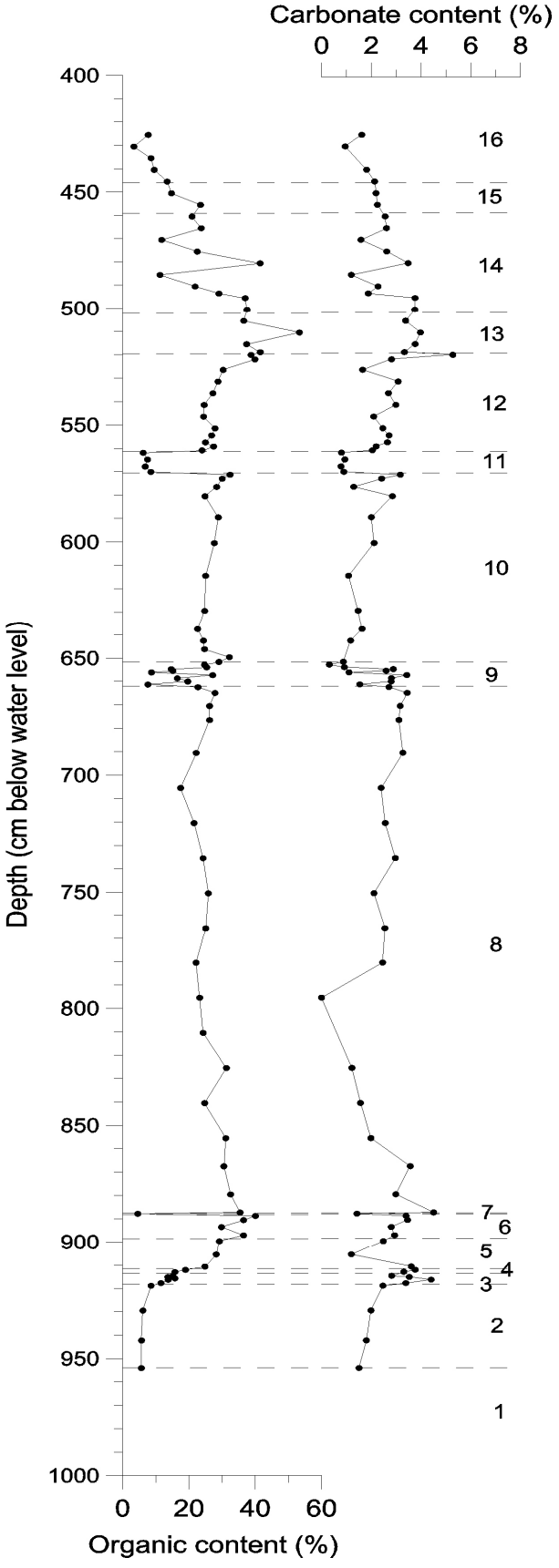

Figure 9. Organic and carbonate content in the Ta4 sediment sequence. Unit numbers are displayed to the right.

5.4 Element variation

Three different parts of the sediment sequence were selected for XRF-scanning, including the isolation, transgression and the three grey minerogenic rich units (7, 9 and 11). The XRF-scanner was set to record 23 different of the, in general, most common elements. As the elements occur in different amounts, the changes in the different elements are more or less likely to be statistically recorded in the sequence. However, most of the elements show a pronounced difference across lithological boundaries. The elements recorded to have about 30 counts per second or more (except Ta and W) are presented in Figure 10, 11 and 12 and are considered further. All the elements recorded are presented in Appendix 1. The scanning was performed at the back of the core while the description was made from the front. This can explain why the unit boundaries not always follow the element variations due to, for example dipping sediment layers.

5.4.1 The supposed isolation sequence and unit 7

The first scanned sequence at 935 to 880 cm depth corresponds to parts or all of unit 2 up to 8 (Fig. 11). Most of the elements (Ar, K, Ca, Ti, Mn, Fe, Zn, Sr) show a gradual decrease from about 923 cm depth. Si starts to decrease later at about 917 cm depth. The amounts of these elements show a stronger fluctuation between 917 and 911 cm depth (approximately unit 3 and 4), with a decreasing trend, reaching more low and stable values in the beginning of unit 5. Sulphur also fluctuates in unit 3, but show low values only from unit 4 and upwards. Several of these elements have previously shown to decrease at isolation boundaries (Sparrenbom *et al.* 2006b). The values for these elements stay low through the rest of the scanned sequence with the exception of a peak in most of these elements at 888 cm, which corresponds to the thin layer of gyttja clay in unit 7.

In contrast, Br and Cu show a general increase throughout the sequence, starting at 923 and 917 cm depth, respectively. There the higher values are stabilized at about 911 cm, corresponding to the beginning of unit 5, and stays high throughout the sequence, except a small dip at 888 cm corresponding to unit 7.

The counts of Zr gradually decreases between about 917 to 907 cm. Cl and Rb do not show any recognizable trend in this sequence. The Si/Ti ratio calculated increase in value from the beginning of unit 5, possibly indicating increasing biogenic silica.

5.4.2 “The grey layers” in units 8-10.

The second scanned sequence at 645 to 675 cm depth corresponds to unit 9 and parts of the surrounding units 8 and 10 (Fig. 10). The elements S, Ar, Cl, K, Ca, Ti, Fe, Zn, Rb, Sr and Zr increase at the same level as the lithological change described as an increasing

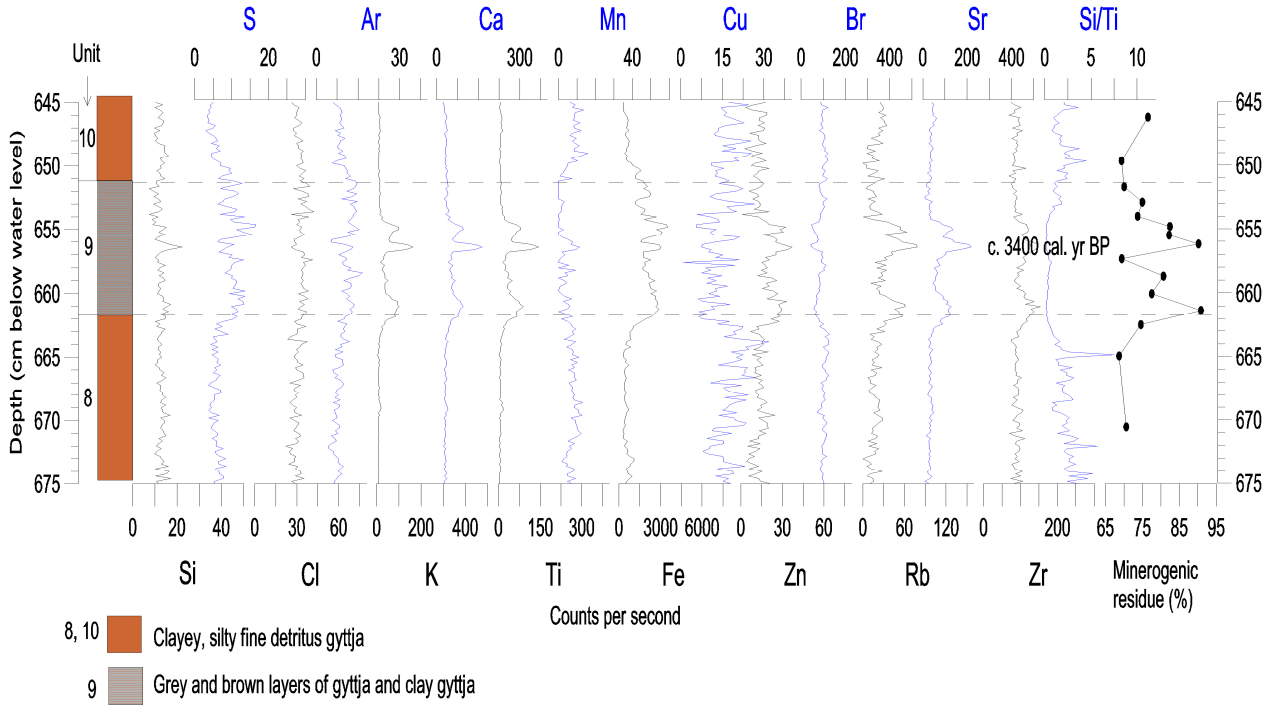

Figure 10. Simplified core log, XRF measured elements, Si/Ti ratio and minerogenic residue for site Ta4 (unit 9 and parts of units 8 and 10). The scale for the black curves is displayed below and the scale for the blue curves is dispalyed above. An AMS-date from the middle part of unit 9 is also shown i the figure.

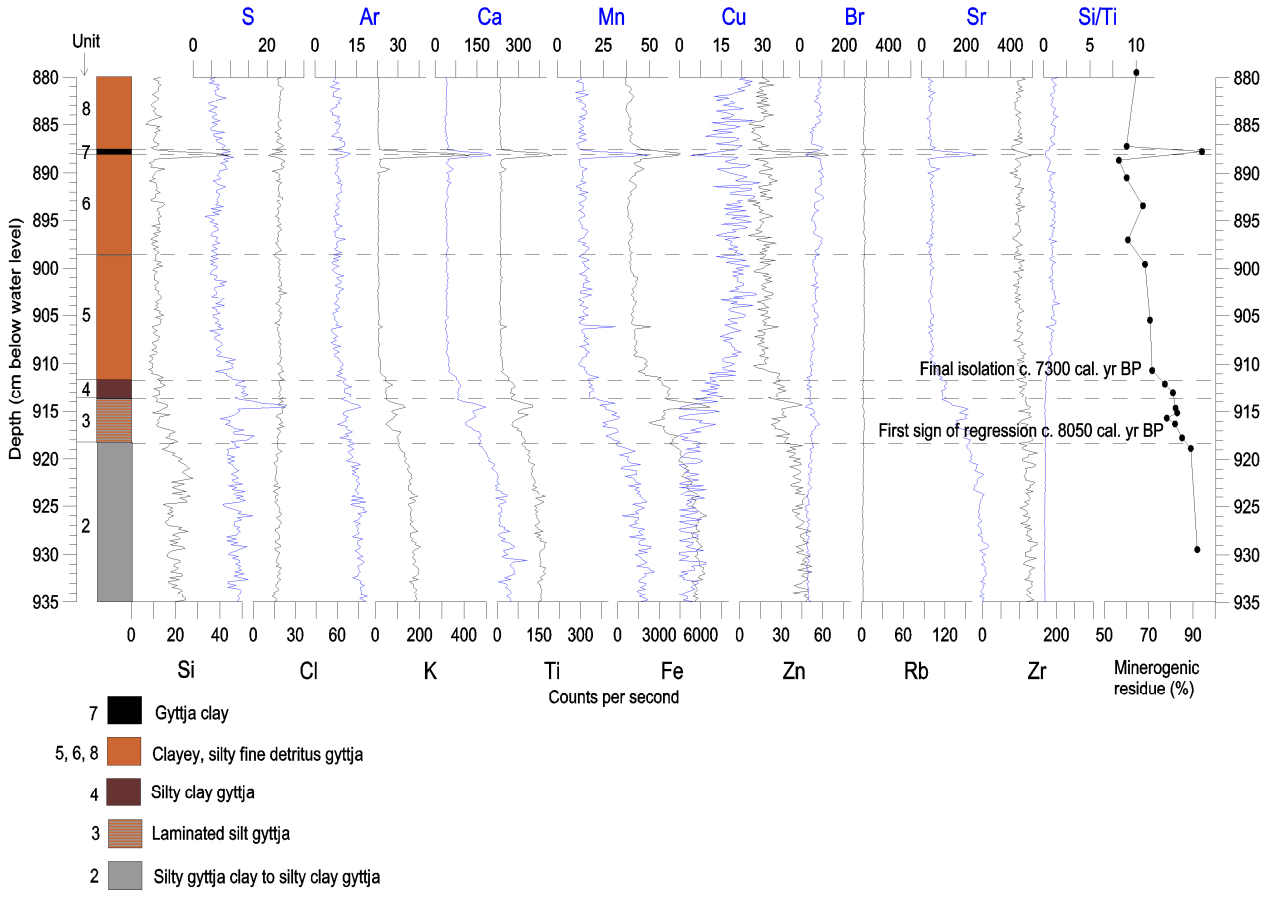

Figure 11. Simplified core log, XRF measured elements, Si/Ti ratio and minerogenic residue for site Ta4 (units 3-7 and parts of units 2 and 8). The scale for the black curves is displayed below and the scale for the blue curves is dispalyed above. AMS-dates from the lower part of unit 3 and lower part of unit 5 are also shown in the figure.

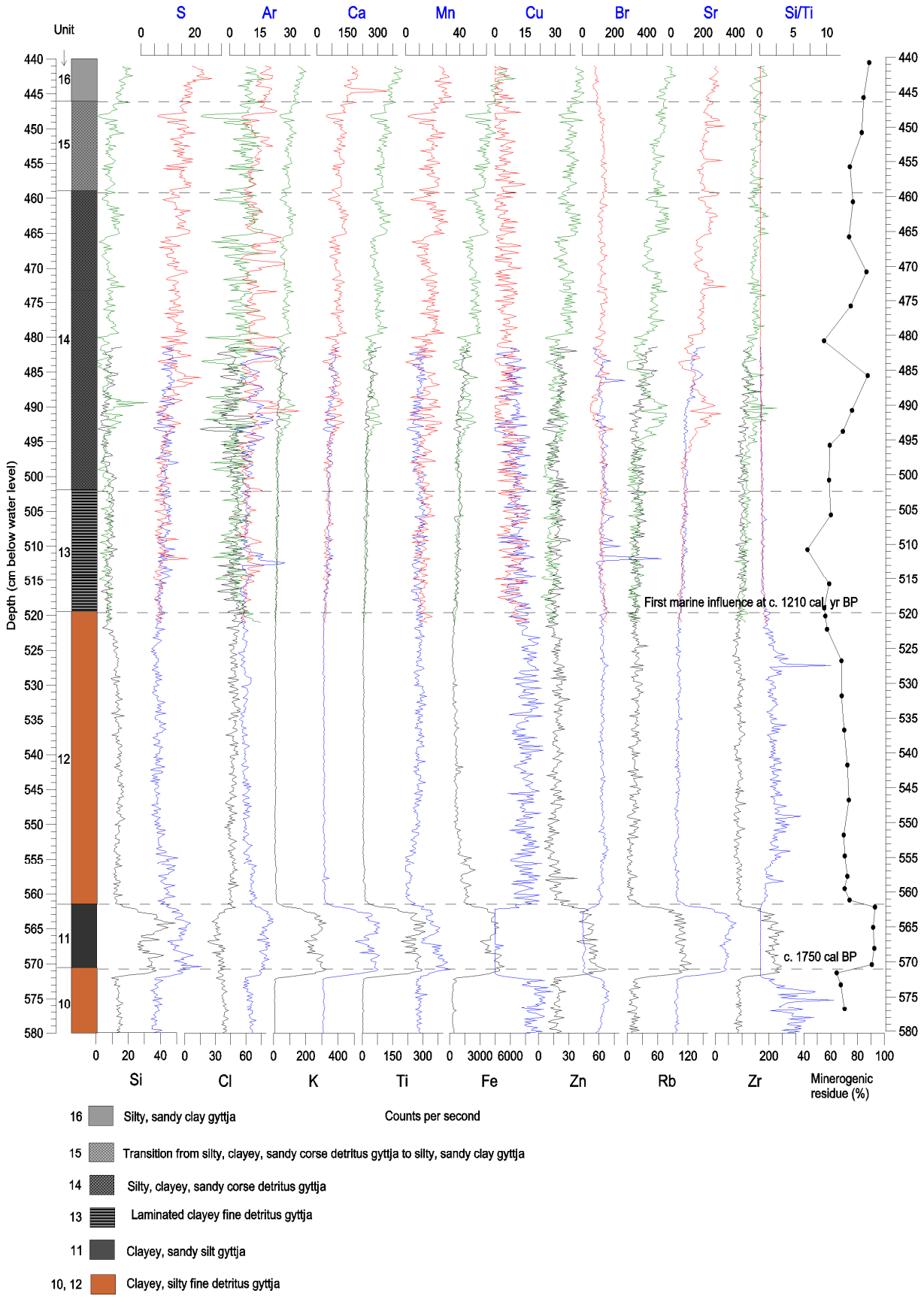

Figure 12. Simplified core log, XRF measured elements, Si/Ti ratio and minerogenic residue for site Ta4 (units 11-15 and parts of units 10 and 16). The different colours of the curves represent two overlapping cores. The scale for the black/green curves is displayed below and the scale for the blue/red curves is dispalyed above. AMS-dates from the lower part of unit 11 and from the lower part of unit 13 are also shown i the figure.

concentration of minerogenic matter. These elements are therefore interpreted to be important constitutes of the mineral material.

As a contrast, Mn, Cu and Br decrease in counts when crossing into unit 9. Si does not show any recognizable trend in this sequence. The Si/Ti ratio is close to zero in unit 9 while higher in the surrounding units.

5.4.3 Grey unit 11 and the supposed transgression

The third scanned sequence stretching from 581cm to 441 cm depth corresponds to unit 11, 12, 13, 14, 15 and parts of unit 10 and 16 (Fig. 12). The sequence includes the distinct grey silt gyttja and the transition from fine detritus gyttja to grey clay gyttja. Since the sequence stretches across two different parallel core sections, the scanning was divided in two, with an overlap between 521 cm and 481 cm. The differences between the cores can be explained by local differences (heterogeneities) and are of course recorded by the XRF-scanner.

The concentrations of most of the scanned elements (Si, S, Ar, K, Ca, Ti, Mn, Fe, Zn, Rb, Sr, Zr) increase to distinctly higher values in the grey silt gyttja (unit 11). As the variability of these elements follows the minerogenic residue curve, they are thought to change in response to the minerogenic content. In contrast, Cl, Cu and Br drop to distinctly lower values in unit 11. The Si/Ti ratio drops to almost zero with higher values in surrounding units.

The supposed transgression in the upper part of the sequence, changing from fine detritus gyttja to clay gyttja, shows a greater variability for the elements analyzed. This is probably due to the heterogeneity of the units, but there is a clear trend. The first change starts with slightly higher values in the beginning of unit 13 for the elements S, K, Ca, Ti, Fe, Sr and Zr. This rise occurs despite the fact that the minerogenic content decreases, and can therefore not be interpreted as a response to the minerogenic content.

Slightly lower values are registered for the two elements (Si, Cu) and six elements (Cl, Ar, Mn, Zn, Br, Rb) do not show any recognizable trends in unit 13. The Si/Ti ratio is almost zero at the beginning of this unit and stays low throughout the rest of the sequence, without any further clear change in biogenic silica.

From unit 14 to 16, the minerogenic content increases and most of the elements show some kind of variation throughout these units, either a marked increase (S, K, Ca, Ti, Fe, Sr, Zr, Cl, Ar, Mn, Zn, Rb) or decrease (Cu). Si and Br continue to show low values.

Most of the elements also show an increase in counts close to the beginning of unit 16. Br however, decreases in the lower part of unit 16 for the first time since the beginning of the transgression sequence, while Cu decreases further. Note that Si starts a decreasing trend at the start of unit 13 and increase again in unit 16.

5.4.4 The complete sequence

The elements whose variability more or less follows the minerogenic content throughout the sequence are S, Ar, K, Ca, Ti, Fe, Zn, Sr, Zr. Mn follows the minerogenic content in the sequence except in unit 9, where it deviates and decreases. Cl shows no direct correlation to the minerogenic content. Cu is always low in counts where the minerogenic content is high. Br shows low counts where the minerogenic content is high except in units 14 and 15. Si shows a rise in some parts where the minerogenic content rises but not in all cases. Rb seems to follow the same trends as the minerogenic content except in unit 2-7, where it is almost absent.

In summary, S, Ar, K, Ca, Ti, Fe, Zn, Sr, Zr always increase and Cu always decrease in the more minerogenic rich units. The changing minerogenic content seems to be one of the most important signals for the element concentrations detected by the XRF-scanner. There can of course be other signals, but these are more difficult to detect. Cu has previously been related to organic matter (Sparrenbom *et al.* 2006b).

The variability of the other elements (Si, Cl, Mn, Br, Rb) is more difficult to explain. In the lowermost and the uppermost units, which are interpreted as marine, none of the remaining elements show similar or correlating trends. This shows that a marine signal is difficult to detect from these. However, in unit 13 the elements S, K, Ca, Ti, Fe, Sr and Zr rise in counts despite a decrease in minerogenic content. The common elements in marine sediments, Ca, Fe, Sr, K and Ti (Böning *et al.* 2007), constitute five of these seven elements, suggesting that these elements instead have a marine origin. Slightly lower values are in the same unit shown for the elements Si and Cu. The rise in organic content can be due to erosion of terrestrial mosses and the decrease in Si could possibly be explained by a lower biogenic silica production.

5.5 Macrofossil content

The units interpreted to be related to the isolation and transgression as well as the three grey units 7, 9 and 11, were analysed regarding their macrofossil content including parts of units just above and below. Samples between 954 cm and 868 cm and from 690 cm to 425 cm were cut out in different intervals, depending on lithological changes. Sample thickness varied between 0.3 cm and 1.9 cm with a volume between 0.3 ml and 4.9 ml, depending on the different layers thicknesses. The macrofossil content for the different intervals investigated are presented in Figure 13-17, in numbers per milliliter and sampling depth for each sample marked by its midpoint. Pictures of identified fossils are shown in Appendix 2a-d.

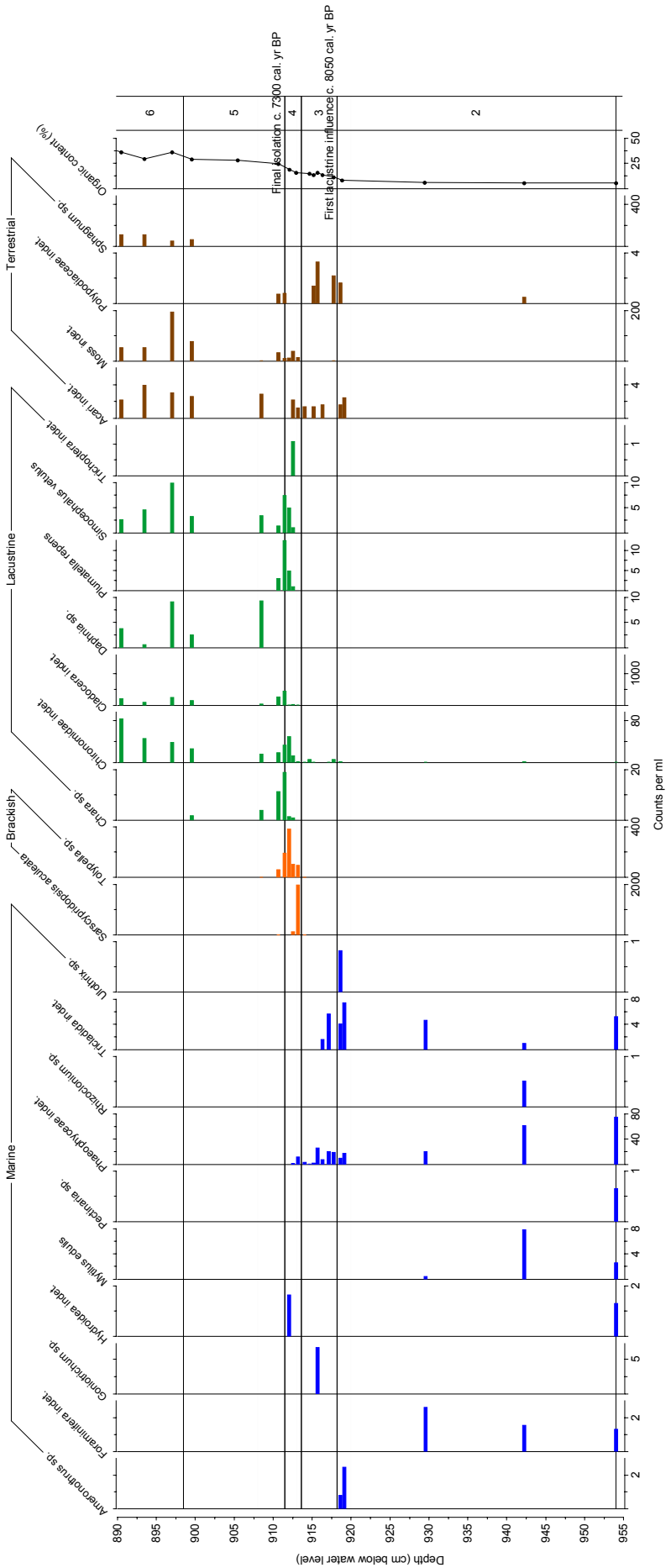

Figure 13. Macrofossil diagram showing the results from the macrofossil analysis in units 3-5 and parts of units 2 and 6. The organic content is also shown. Unit numbers are displayed to the right. Note the different scale for the different taxa. AMS-dates for the supposed first lacustrine influence and the final isolation are also displayed.

5.5.1 Supposed isolation (unit 3 and 4)

The lowermost 3 units in the sediment sequence contain very few macrofossils, making it difficult to identify any clear difference in macrofossil content between these units (Fig. 13). However, ten different identified marine taxa confirm the marine origin of the sediments.

In unit 1 to 3 macrofossils of the taxa *Ameronothrus sp*., Foraminifera indet., *Goniotrichum sp.*, Hydroidea indet., *Mytilus edulis*, *Pectinaria sp.,* Phaeophyceae indet., *Rhizoclonium sp*, Tricladida indet. and *Ulothrix sp*. are found, and they all suggest marine depositional conditions. Exceptions are a few individuals of the lacustrine taxa Chironomidae indet. and three terrestrial macrofossils. These can, however, easily be explained by surface runoff.

Most of the lacustrine macrofossils start to appear in the lower part of unit 4: *Chara sp*., Cladocera indet., *Plumatella repens*, *Simocephalus vetulus* and Trichoptera indet., suggesting an increased fresh water influence. Chironomidae indet. increases in numbers from this level and *Daphnia sp*. appears for the first time in unit 5. The brackish indicators *Sarscypridopsis aculeata* and *Tolypella sp*. are the dominating macrofossils in the lower part of unit 4 with only *Tolypella sp*. extending into unit 5. No marine fossils are found above unit 4 in the lower part of the sediment sequence.

A few terrestrial taxa are present in units 2-5 (Acari indet., moss indet. and Polypodiaceae indet. and *Sphagnum sp*.), where only moss indet. shows a marked variability with a rise in numbers at the lower part of unit 4.

The macrofossil content suggests a transition from marine to brackish conditions at the boundary between unit 3 and 4, contrary to the element concentration and organic content that suggest the boundary to be situated between units 2 and 3. The macrofossil content also suggests totally lacustrine conditions from the beginning of unit 5, corresponding to the final isolation of the basin.

5.5.2 Gyttja clay (unit 7)

The macrofossil content of the 0.5 cm thick clay rich unit 7 and its surroundings are presented in Figure 14. The macrofossils in unit 7 are composed of mainly lacustrine species, although in reduced numbers compared to the units above and below. A similar trend is shown for the terrestrial macrofossils. Common lacustrine species in this unit are Chironomidae indet., Cladocera indet., *Daphnia sp*., and *Simocephalus vetulus*. Terrestrial macrofossils occur in the form of Acari indet., moss indet. and *Sphagnum sp*. A few brackish indicators such as *Sarscypridopsis aculeata* occur around unit 7 and some possible marine algae occur within unit 7. The macrofossil content in and around unit 7 indicates a lacustrine depositional environment.

5.5.3 Grey layers (unit 9)

Unit 9 consists of about 10 cm of heterogenic layers that shift in colours, element concentration and minerogenic content. The macrofossil content do not seem to vary correspondingly, as no clear differences before, after and between the layers can be seen (Fig. 16). Only lacustrine and terrestrial macrofossils were found in this unit. Lacustrine macrofossils present are *Chara sp*., Chironomidae indet., Cladocera indet., *Plumatella repens*, *Simocephalus vetulus* and Trichoptera indet., where only *Simocephalus vetulus* shows a marked increase in one of the light brown layers. Terrestrial macrofossils include Acari indet., *Betula nana*, Polypodiaceae indet., moss indet. and *Sphagnum sp*., where the two latter show the only distinct increase in the sequence, occurring in one of the grey layers, probably indicating increased erosion. The macrofossil content in unit 9 indicates a lacustrine depositional environment.

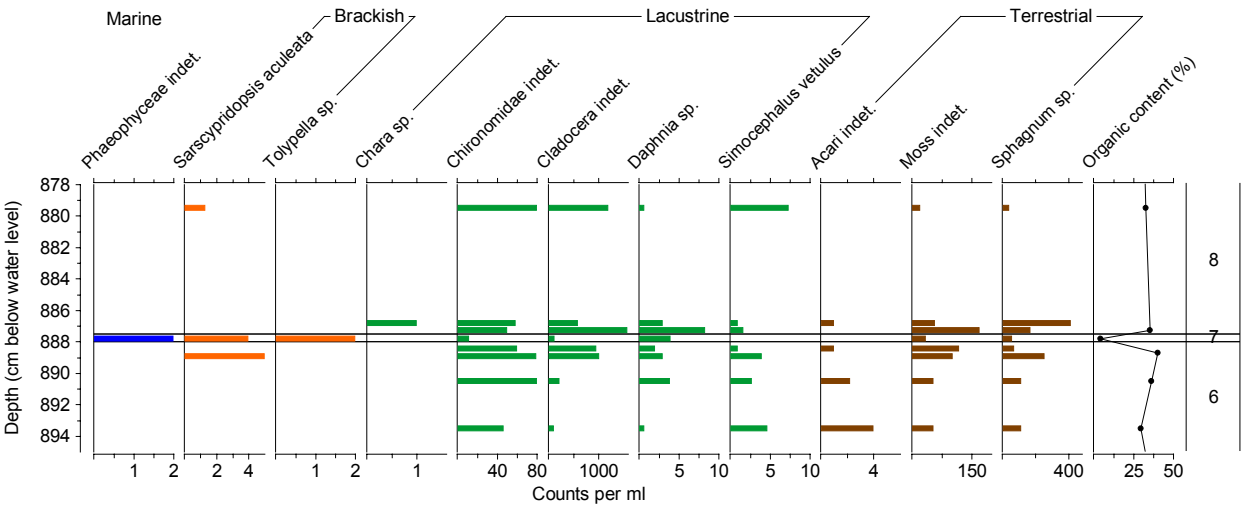

Figure 14. Macrofossil diagram showing the results from the macrofossil analysis in unit 7 and parts of units 6 and 8. The organic content is also shown. Unit numbers are displayed to the right. Note the different scale for the different taxa.

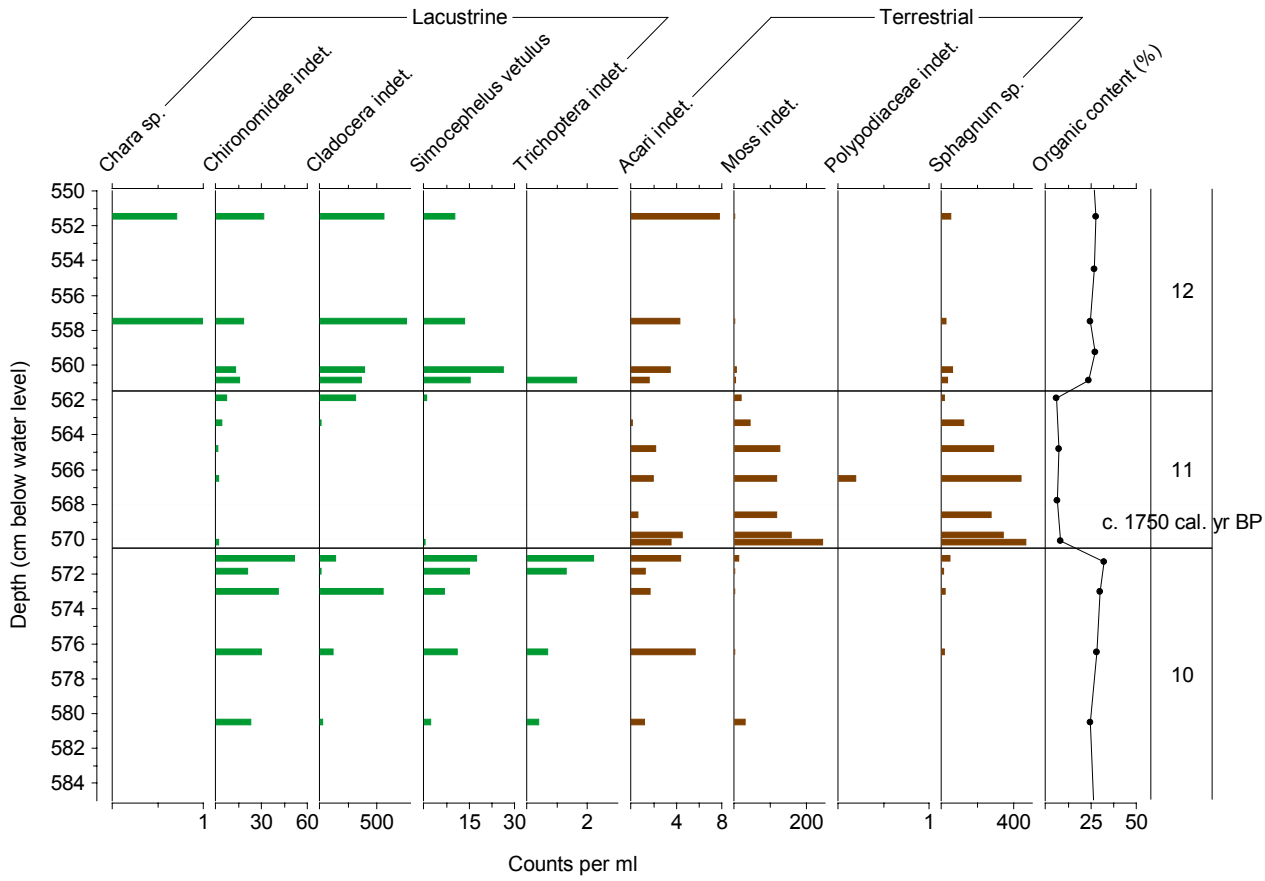

Figure 15. Macrofossil diagram showing the results from the macrofossil analysis in unit 11 and parts of units 10 and 12. The organic content is also shown. Unit numbers are displayed to the right. Note the different scale for the different taxa. An AMS-date from the lower part of unit 11 is also displayed.

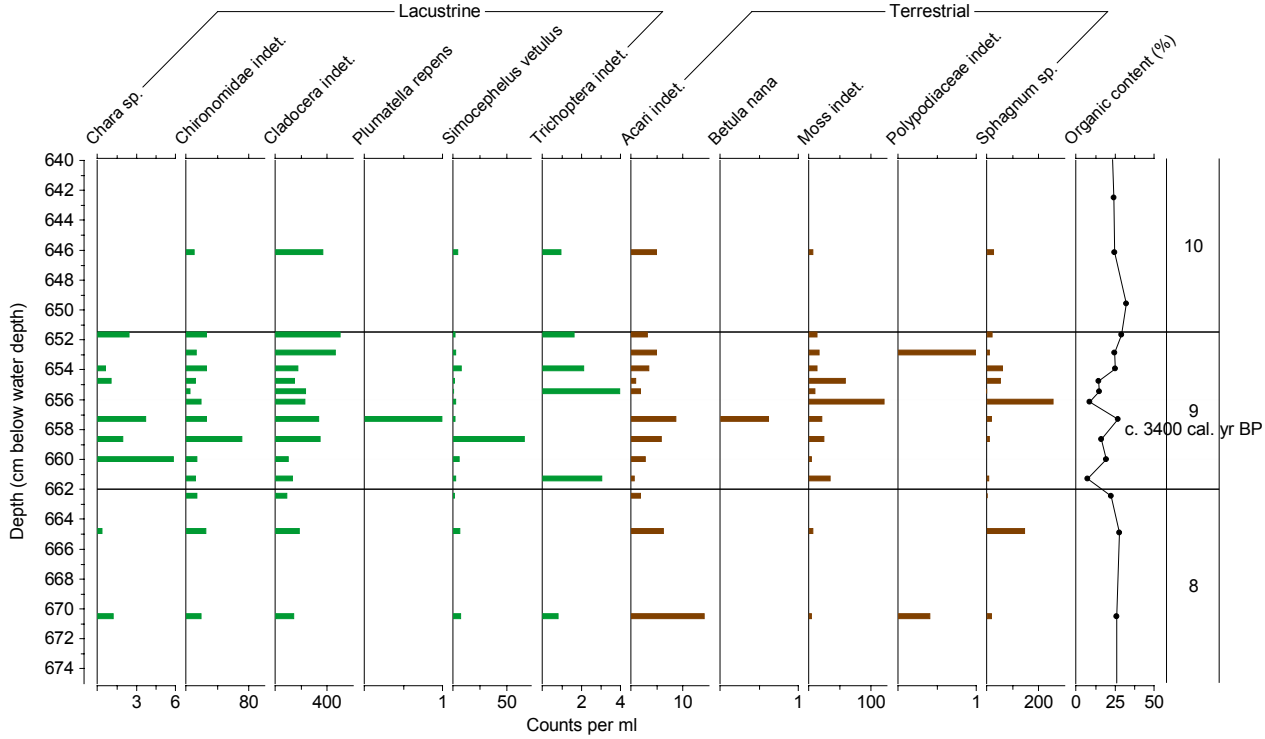

Figure 16. Macrofossil diagram showing the results from the macrofossil analysis in unit 9 and parts of units 8 and 10. The organic content is shown. Unit numbers are displayed to the right. Note the different scale for the different taxa. An AMS-date from the middle part of unit 9 is also displayed.

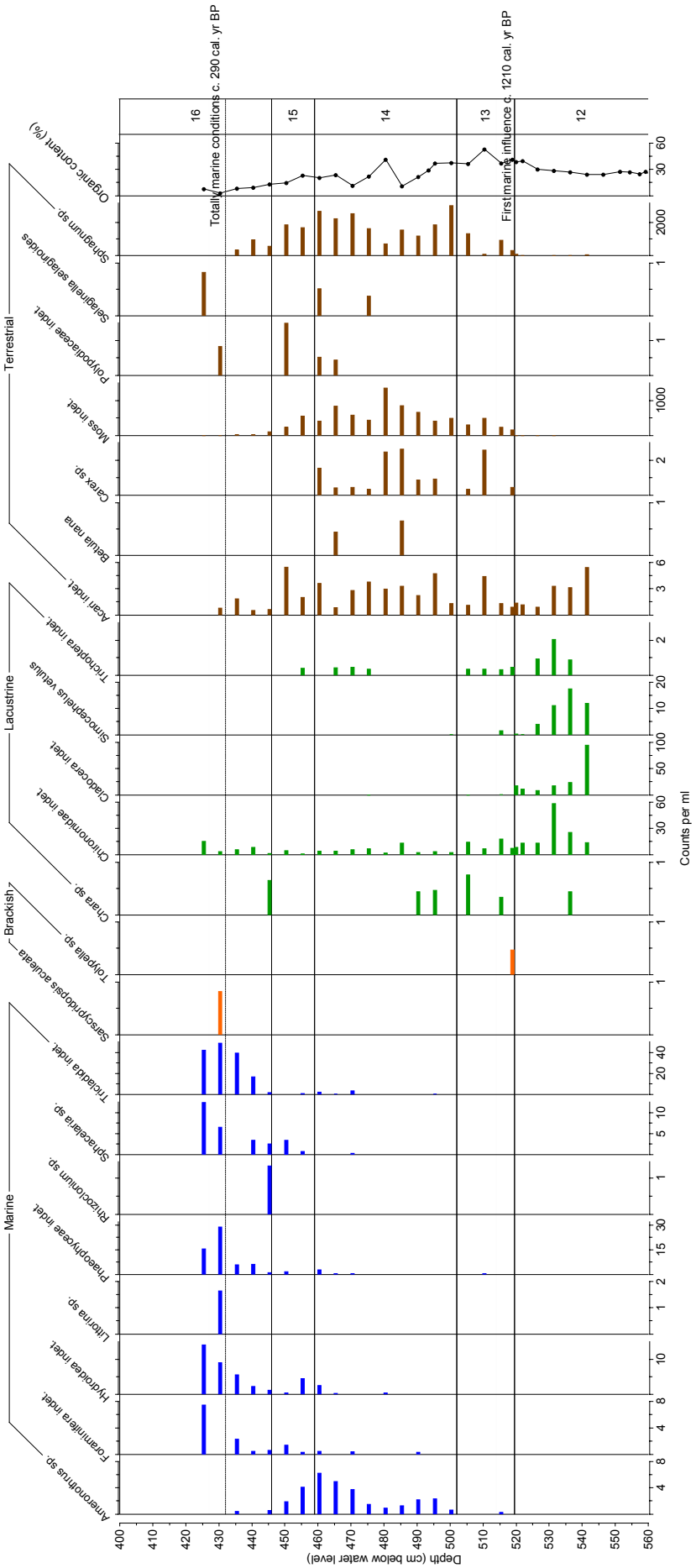

Figure 17. Macrofossil diagram showing the results from the macrofossil analysis in units 13-15 and parts of units 12 and 16. The organic content is also shown. Unit numbers are displayed to the right. Note the different scale for the different taxa. An AMS-date for the supposed first marine influence and an interpolated date for when total marine conditions started to occur are also displayed.

5.5.4 Grey unit 11

This unit is distinct both in lithology, organic content, geochemical signature and in macrofossil content. Only lacustrine and terrestrial macrofossils are found in this unit. The lacustrine macrofossils, Chironomidae indet., Cladocera indet., *Simocephalus vetulus* and Trichoptera indet., show a distinct decrease in unit 11 (Fig. 15). In contrast, the terrestrial mosses show a distinct increase in the lower part of the unit and thereafter a rather gradual decrease towards the top of the unit. The increase of terrestrial macrofossils indicates increased erosion. The macrofossil content in unit 11 shows a lacustrine depositional environment.

5.5.5 Supposed transgression (units 13, 14, 15, 16 and 17)

The transition from fine detritus gyttja to clay gyttja in top of the sediment sequence covers about 75 cm, i.e. several units. The fine detritus gyttja in unit 12 contains mostly lacustrine macrofossil species, but a few terrestrial remains are also found (Fig. 17). The lacustrine macrofossils decrease in numbers in the top of unit 12. Cladocera indet. and *Simocephalus vetulus* disappear in unit 14, while Chironomidae indet. can be found in small numbers throughout the unit. The terrestrial macrofossils like mosses in general and *Sphagnum sp*. in particular show a distinct increase while *Carex sp*. appear for the first time in the sedimentary sequence in the lower part of unit 13.

The terrestrial macrofossils dominate in units 13-15 and decrease in the upper part of unit 15 and continue to exist in low numbers in unit 16. A few marine macrofossils appear in unit 13 with increased diversity in unit 14 and 15. Foraminifera indet., Hydroidea indet., Phaeophyceae indet., *Sphacelaria sp*. and Tricladida indet. increase in numbers in the lower part of unit 16, while *Ameronothrus sp*. is present in high numbers in unit 14 and 15. The higher counts of terrestrial mosses in units 13-15 indicate increased erosion.

The macrofossils in unit 12 that indicate a lacustrine depositional environment decrease in numbers in unit 13 where also the appearance of marine taxa starts, indicating some marine influence in this unit. By adding the marked increase in erosion shown by the increase in terrestrial macrofossils that is thought to accompany a transgression, the first marine influence in the basin is suggested to be recorded in the boundary between units 12 and 13.

Since the marine macrofossils continue to increase in numbers in the beginning of unit 16, the transition into fully marine conditions are probably found in this unit. Somewhere between 435 cm and 430 cm, the marine macrofossils seem to have stabilized at higher numbers and the amount of terrestrial macrofossils have decreased. The macrofossils are therefore interpreted to indicate fully marine conditions, the same conditions that occur today, at a depth of *c.* 432 cm.

Table 3. AMS radiocarbon and calibrated dates for site Ta4

Lab. no.	Depth (cm)	Age ^{14}C BP	Calibrated age BP 2σ (95.4%)	Midpoint cal. yr BP 2σ	Comments	Material
LuS7520	916.9-918.1	7200 ± 60	7930-8170	8050	Just above the first sign of isolation (unit 3)	Moss
LuS7521	910.2-911.2	6405 ± 60	7170-7440	7305	Just above the final isolation (unit 5)	Brown moss
LuS7522	656-658.9	3185 ± 60	3260-3570	3415	In the middle of unit 9	Brown moss, *Sphagnum sp*., *Betula nana* seed
LuS7523	569.5-570.4	1840 ± 50	1620-1890	1755	In the lower part of unit 11	Brown moss, *Sphagnum sp*.
LuS7524	518.5-519.4	1320 ± 55	1080-1340	1210	Just above first sign of the transgression (unit 13)	Brown moss, *Sphagnum sp*.
LuS7525	446-447	1555 ± 50	1340-1550	1445	Above the transgres-sion sequence (unit 16)	Brown moss, *Sphagnum sp*.
LuS7607	442.5-444	2225 ± 50	1420-1910	1665	Above the transgres-sion sequence (unit 16)	Clay gyttja

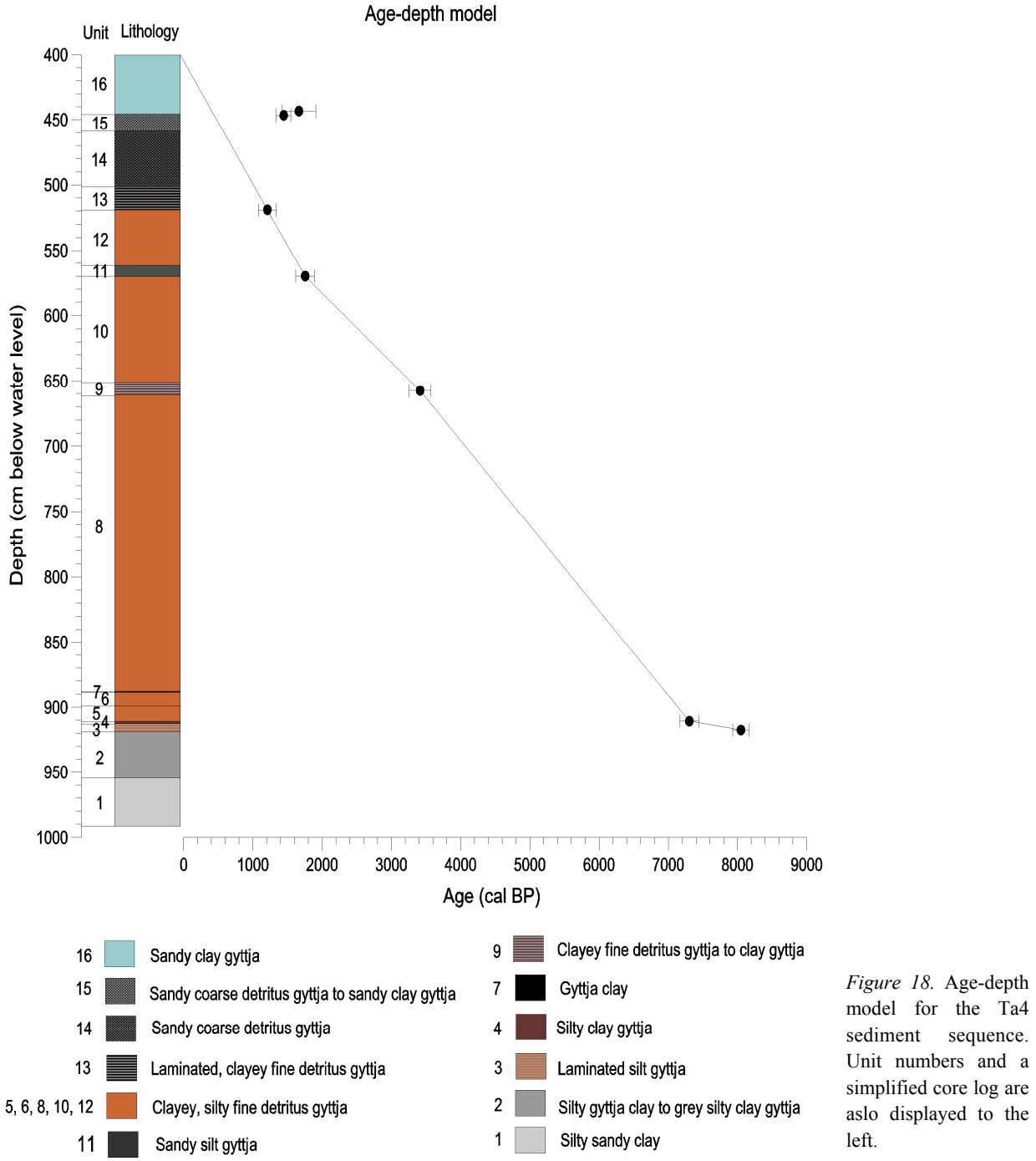

Figure 18. Age-depth model for the Ta4 sediment sequence. Unit numbers and a simplified core log are aslo displayed to the left.

5.6 Dating

Six terrestrial macrofossil samples and one bulk sample were picked out for radiocarbon analysis. Two samples were taken from the isolation sequence and three from the units showing the transgression, and one from each of the more minerogenic units 9 and 11. At the isolation one sample was taken from the lower part of unit 3 where the lamination starts and one in the lower part of unit 5, where the lacustrine macrofossils start to dominate. In the transgression sequence, one sample was taken in the lower part of unit 13 where the terrestrial macrofossils begin to dominate and two in the lower part of unit 16. All ages obtained are presented in Table 3 and an age-depth model is presented in Figure 18.

The two uppermost dates are thought to be too old as they are both older than the sample taken 75 cm further down in the sequence. This can be explained by the fact that previously deposited material from other parts of the basin have been eroded and transported to the centre of the basin. The dates represent ages for different steps in the development of the basin, i.e. the isolation and transgression, but also when the minerogenic units in the centre of the core were deposited. The sedimentation rates range between 0.091 mm $year^{-1}$ in the bottom of the sequence to 0.98 mm $year^{-1}$ in the top of the sequence.

6 Discussion

6.1 Basin development

6.1.1 Oldest sediments

The first two units in the sediment sequence have been deposited in a marine environment, indicated by lithology, marine macrofossils, high minerogenic content and the geochemistry. However, the elements measured start to change already in the top part of unit 2, but since the organic content is almost constant, the conditions are interpreted to be similar throughout the unit. The dating in the lower part of unit 3, together with the age-depth model, suggests that the marine environment in the basin lasted until *c.* 8000 cal. yr BP. The sea level must have been at least 3.5 m higher than the threshold when units 1 and 2 were deposited, corresponding to a relative sea-level above 0.0 m a.h.a.t. (see conditions in Fig. 5a).

6.1.2 Isolation

The first sign of a shallow basin is indicated by the laminated sediments of unit 3. At the same level the organic content increases and the counts of the measured elements continue to change markedly. However, no change in the macrofossil content can be seen. It is still characterized by a marine flora and fauna. The sediment level where the basin is interpreted to have been cut off from the sea during lowest tide, is set to the boundary between units 2 and 3. This is based on the laminations, organic content and the geochemical changes. Even if the marine water did not reach above the threshold during the lowest tide, marine conditions in the basin could still dominate, explaining the marine macrofossils deposited. The laminated sediments suggest a stratification of the basin with fresh and marine water at different water depth. Fresh water from ground water and/or surface runoff is interpreted to have started to influence the basin at this time, at the same time as the marine water inflow was reduced.

The change from marine to brackish conditions corresponds to the conditions in Figure 5b, when sea level was at a position 3.5 m higher than the threshold (0.0 m a.h.a.t.), which coincides with a relative sea-level at the same elevation as today. The dating of the lower part of unit 3 to 8050 cal. yr BP is interpreted to represent this boundary, and is inserted as a point in the relative sea-level curve (Fig. 19). However, the possibility to exactly distinguish this boundary in the sediment can be somewhat questioned, as it is not totally certain when the lacustrine influence starts to effect the basin environment.

Several lacustrine macrofossils start to appear in unit 4 together with a few brackish species, which indicate increased fresh water conditions in the basin. The organic content continues to increase and most element counts continue to change throughout this unit.

In the lower part of unit 5, the element counts and the organic content stabilizes at more constant values. The brackish macrofossils have almost disappeared, no marine species are found and the lacustrine macrofossils dominate in the sediments above this level. This indicates that the marine water had ceased to enter the basin even at the highest tides, corresponding to a relative sea level at 3.5 m b.h.a.t. This boundary between unit 4 and 5 is interpreted to represent the level of the final isolation (see illustration in Fig. 5d). The dating from the lowermost part of unit 5 to *c.* 7300 cal. yr BP, just above this boundary, is interpreted to represent the age of the final isolation and is inserted as a point in the relative sea-level curve (Fig. 19).

The time span between 8050 and 7300 cal. yr BP corresponds to 750 years of brackish conditions in the basin, recorded in a 6.7 cm long sediment interval. During these 750 years the relative sea level fell 3.5 metres (see Fig. 5c), corresponding to the height difference between the lowest and highest astronomical tide in the area.

6.1.3 The middle part of the sedimentary sequence

Between 911.5 cm and 519.5 cm depth (dated to *c.* 7300 and 1200 cal. yr BP), the sediment sequence is characterised by lacustrine deposition, suggesting that the relative sea level stayed below 3.5 m b.h.a.t during this interval (see Fig. 5e). The element counts, the organic content and the macrofossil flora and fauna all support similar conditions during the entire period. However, three units (7, 9 and 11) in this interval deviate in lithology, organic content, element counts and macrofossil content.

The 0.5 cm thick gyttja clay layer (unit 7) is interpreted to have been deposited during one single event as it is massive and thin. The clayey material of this unit could have been transported to the basin during heavy rainfall or spring flood. This could e.g. have happened during a spring flood with lake ice still in the basin, which could give calm sedimentation conditions. In spite of the fact that almost no marine macrofossil was found in the unit, erosion originating from a storm event when the sea level was close to the threshold can not be excluded.

Units 9 and 11 cover about 10 cm intervals each and are interpreted to have been caused by increased erosion, possibly deposited during periods of climatic change in the region. The ages of these units are around 3400 and 1750 cal. yr BP, respectively. If the sedimentation rate was constant in the middle of the sedimentary sequence, which is doubtful, the deposition time of unit 9 and 11 was about 160 and 140 years, respectively.

The deposition of unit 9 and 11 are within the period of more unstable climate recorded from 3700 cal. yr BP (Andresen *et al.* 2004). The two dry periods (3700-2400 cal. yr BP and 1800-600 cal. yr BP) recorded by Andresen *et al.* (2004) coincide somewhat

with the age of units 9 and 11, but arid conditions would suggest the opposite to increased erosion. More humid conditions are suggested by Fredskild (1973) between *c.* 3900 and 1900 cal. yr BP, which could explain increased erosion when unit 9 was deposited. However, unit 11 does not coincide with these wetter conditions.

Unit 9 and 11 could also have been deposited during single heavy rainfalls, spring flood, sea-level rise, slope processes or increased storminess when the sea level was close to the threshold elevation.

According to this investigation the minerogenic units in the middle of the sediment sequence can not be used as sea-level indicators. However, the geochemical analyses from these units show element counts comparable to those in the marine units in the top and bottom of the sediment sequence. The element counts recorded in the XRF-scanning must therefore mainly reflect the minerogenic content rather than a marine influence. Further analyses of these units, including diatom content, could possibly aid in interpreting the depositional environment.

6.1.4 Transgression

From the stable sedimentation registered in the middle part of the sedimentary sequence, lithology, element counts, organic content, and macrofossil content start to change in the lower part of unit 13. This is probably the first sign of a marine influence when the sea was connected to the basin at highest tide. The boundary between units 12 and 13 then represents the conditions illustrated in Figure 5d. Terrestrial macrofossils dominate in units 13-15 and thereby suggest a increased degree of erosion. Increased erosion is expected during a transgression, as tidal current flows in and out of the basin twice a day. During the period when the basin was isolated from the sea, terrestrial mosses could have grown on and around the threshold and on the shores, becoming a sediment source of terrestrial material eroded and deposited during the sea level rise. The laminated sediment in unit 13 could have been formed due to the stratification of fresh and marine water in the basin. A complication of the interpretation of the lowermost unit 13 as the start of the transgression, is the absence of marine macrofossils and the increase in organic matter. However, abundant marine macrofossils are not expected as it is the first marine influence we seek and marine water rarely entered the basin during this first stage. The increase in organic content could possibly be explained by a favoured organic production due to the nutrients transported from the marine water to the basin during the highest tide. Also the high amount of eroded terrestrial macrofossils could cause an increase in the organic content in the sediment.

The high amount of terrestrial macrofossils could also be explained by an overgrowth of the basin into a fen-like or bog-like environment. However, if no substantial compaction of the sediment has occurred, the fen or bog would have been situated below the ground water level, which seems unlikely.

The boundary between units 12 and 13 is interpreted to constitute the level where the marine water started to reach into the basin during the highest astronomical tides, which corresponds to a relative sea level at 3.5 m b.h.a.t. A radiocarbon dated sample from the lower part of unit 13 gives an age of *c.* 1200 cal. yr BP and is interpreted to correspond to a relative sea level 3.5 m b.h.a.t. and is plotted in the sea-level curve in Figure 19.

Today, the basin is connected to the sea even during the lowest tides and this situation is illustrated in Figure 5B. The time when these conditions began corresponds to when the sea level reached its present level at Tasiusaq. The boundary between units 15 and 16 is very gradual, and there is no visible change above 446 cm depth. However, the element counts change and the organic content increase throughout unit 16. Also, the marine macrofossils seem to continue to increase to about 432 cm depth, at the same time as the terrestrial macrofossils decreased markedly. Therefore the level recorded in the sediments at which the basin is connected to the sea even at the lowest tide is set to 432 cm depth, corresponding to a relative sea level at 0.0 m a.h.a.t. These conditions prevailed until today if relative sea-level has been constant. At least no change is visible in the sediment above this depth. Since the two dates from about 445 cm depth are considered to be too old because of reworking, the age when these conditions started, have been calculated by interpolation in the age-depth model. The age given for the level at 432 cm depth was calculated to 290 cal. yr BP, with an uncertainty estimate of ± 200 years, and is used in the relative sea level curve in Figure 19.

The transgression sequence covers 88 cm of sediment deposited during approximately 900 years, corresponding to a sea level rise of 3.5 m, from when the first marine water entered the basin during the highest tides to when the basin was part of the sea even at lowest astronomical tide. During this interval, the situation is considered to be the one illustrated in Figure 5c.

6.1.5 Youngest sediment

The uppermost part of the core is thought to represent a similar depositional environment as today, also comparable to that in the bottom of the core. These conditions were reached some time during the last 500 years.

6.2 A sea-level curve from the Tasiusaq area

Radiocarbon dates of the time when sea level was situated at the threshold level of the Ta4 basin are used here to construct a new relative sea-level curve from the Tasiusaq area (inner Bredefjord). By adding results from Randsalu (2008) the relative sea-level curve has been extended further back in time. The data used are

shown in Tables 5 and 6, and the sea-level curve is presented in Figure 19. The horizontal error bars correspond to the 2σ error range for the AMS-dates, alternatively estimates from interpolation. The vertical error bars correspond to the calculated total height uncertainty.

6.2.1 Minimum deglaciation age

The oldest calibrated ^{14}C age obtained in this study is *c.* 8050 cal. yr BP and a date from Randsalu (2008) shows an age of *c.* 8750 cal. yr BP. These dates suggest a minimum deglaciation age for the study area to be sometime before 9000 cal. yr BP. A date from Fredskild (1973) shows an age of *c.* 9500 cal. yr BP and indicates a similar minimum age. One anomalous old date shows an age of *c.* 11250 cal. yr BP (Sparrenbom *et al.* 2006b), which indicates a much earlier deglaciation. Models by Sparrenbom *et al.* (2006b) suggest a deglaciation before 10500 cal. yr BP.

Most of the dates above are well within the Holocene, which implies that the warmer climate possibly caused the ice sheet to retreat during several thousands of years before this time. The oldest date obtained from the outer coast shows an age of *c.* 13 800 cal. yr BP (Bennike *et al.* 2002). Compared to the inner Bredefjord, this suggests a deglaciation of about 100 km in the Julianehåb district in about 3000 years.

6.2.2 The Marine Limit (ML)

Some features that might indicate the marine limit was measured during fieldwork (Table 4). The highest lake found in the inner Bredefjord area with a certain isolation (Ta2), is situated at about 31 m a.h.a.t. and lakes without any clear isolation (Ka1 and Ka2) are situated at 42 and 54 m a.h.a.t. (Ole Bennike, personal communication), which suggests a marine limit between 31 and 42 m a.h.a.t. A raised beach ridge in the area was measured to 42 m a.h.a.t. and was probably formed during storm events, when the highest astronomical tide was a few metres below. The marine limit is also indicated by possibly wave washed sediments and a terrace measured to 41 m and 42 m a.h.a.t., respectively. A beach ridge at 36 m a.h.a.t. (Fredskild 1973) and a terrace at an elevation of 10-20 m a.h.a.t. (Weidick 1975) adds to these observations, together with a basin without any isolation at *c.* 64 m a.h.a.t. (Fredskild 1973). The marine limit in the Tasiusaq area is therefore suggested to be around 40 m a.h.a.t.

The marine limit in the inner Bredefjord area is similar to the marine limit in both the Nanortalik area (*c.* 32-46 m a.h.a.t. according to Bennike *et al.* 2002), the Qaqortoq area (31-52 m a.h.a.t. according to Sparrenbom *et al.* 2006b), the Narsaq area (33-59 m a.h.a.t. according to Funder 1979) and below 45 m a.h.a.t in the Ipiutaq area (Sparrenbom *et al.* 2006b). However, it would be expected that the marine limit should be higher towards the inland ice and uplift dome where the ice thickness was largest. However, in Greenland a large portion of the ice sheet is still pressing down the crust and the highest marine limit would therefore be expected to be found some distance between today's ice margin and the coast where the ice removal is greatest.

A compilation of the data from Bennike *et al.* (2002), Sparrenbom (2006a, b), Randsalu (2008) and this study is presented in Figure 20. The delay in regression between Qaqortoq and Tasiusaq, and with almost the same marine limits, indicates that ice still covered the Tasiusaq area while a large part of the land uplift occurred. If the Bredefjord area was acting as a major drainage path for the southern Greenland Ice Sheet, as suggested by the eroded landscape and the topography, then the ice sheet thickness in the Bredefjord area must have been relatively thin.

If the relative sea-level curves from Nanortalik, Qaqortoq and Tasiusaq (Fig. 20) are extended up to 40 m a.h.a.t., the approximate marine limit, the uplift since the time the ice disappeared from the different areas can be compared. According to data from Lambeck *et al.* (2001) the global sea level was about 70 m below today in Nanortalik, about 55 m below today in Qaqortoq and about 30 m below today in Tasiusaq when the areas were deglaciated. The total uplift since the deglaciation was then 110 m in Nanortalik, 95 m in Qaqortoq and 70 m in Tasiusaq, also suggesting that most of the uplift in Tasiusaq occurred when the area was still covered by the ice sheet.

Table 4. Marine limit and lower sea level limit indicators in the study area

GPS no.	Lat	Long	Type of measurement	Measured hight m a.h.a.t.
G704	61.13668	314.3488	Saddle to lake Ta1, slightly higher than highest beach ridge	42.4
G708	61.13343	314.3415	Slope break on hillside, possible marine limit	41.0
G711	61.13882	314.3493	Terrace above uncored lake	42.0
G706	61.13897	314.3404	Lake Ta2, Threshold level	31.4
G715	61.07983	314.327	Lake Ka1, Threshold level	42.1
G716	61.0848	314.2896	Lake Ka2, Threshold level	54.2
-	-	-	Marine embayment Nu2, Threshold level, measured with echosounder and estimated from Narsaq predictions	-4.5

Table 5. Ages and uncertainties used in sea-level curve

Basin Code	Age ^{14}C BP	Cal. age BP 2σ (95.4%)	Comments	Interpreted isolation or transgression age (cal. yr BP)	Age uncertainty (years) based on 2σ or estimation	Source
Ta4	7200 ± 60	7930-8170	First sign of lacustrine influence	**8050**	**± 120**	This study
Ta4	6405 ± 60	7170-7440	Isolation age	**7305**	**± 135**	This study
Ta4	1320 ± 55	1080-1340	First sign of marine influence	**1210**	**± 130**	This study
Ta4	1555 ± 50, 2225 ± 50	1340-1550, 1550-1800	Transgression age, interpolated	**290**	**± 200**	This study
Ta1	7590 ± 60, 8355 ± 65	8210-8550, 8780-9290	Isolation age	**8750**	**± 200**	Randsalu (2008)
Ta3	8105 ± 60, 7860 ± 60	8770-9270, 8540-8980	Isolation age	**8500**	**± 200**	Randsalu (2008)

Table 6. Hight and uncertainties for basin thresholds used in sea level curve

Site	GPS nr	Lat / Long	Measured hight m a.h.a.t.	Measured object	Measurement method	Interpreted threshold elevation m a.h.a.t.	Measure-ment uncertainty (m)	Assess-ment of threshold uncertainty (m)	Tidal uncertainty (m)	Total uncertainty (m)	Source
Ta1	G705	61.13897 / 314.3404	26.35	Water level	GPS	**25.8**	0.1	0.1	0.5	**0.5**	Randsalu (2008)
Ta3	G707	61.13596 / 314.3347	12.44	Water level	GPS	**12.2**	0.1	0.3	0.5	**0.6**	Randsalu (2008)
Ta4	-	-	-1.0	Threshold level	Rod	**-3.5**	0.1	0.3	0.5	**0.6**	This study

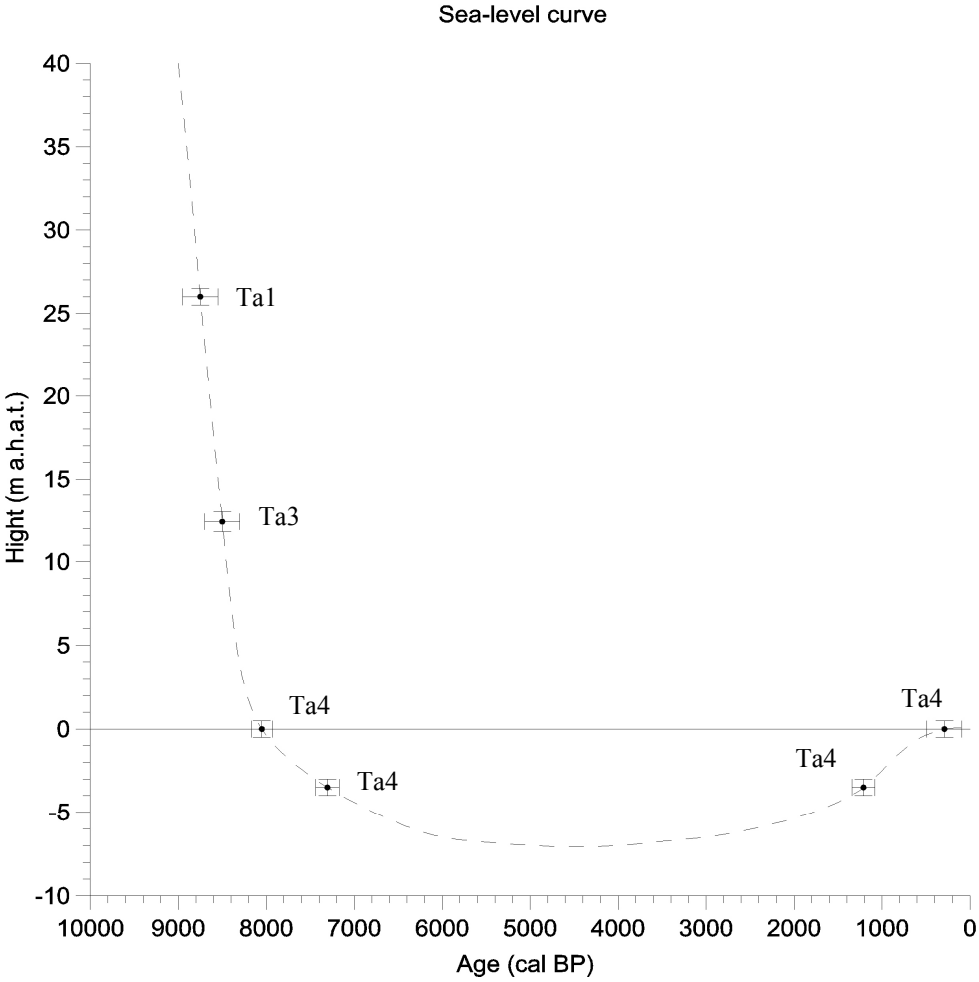

Figure 19. A sea-level curve from the Tasiusaq area. Ages and elevation for Ta1 and Ta3 (Randsalu 2008) and Ta4 (This study).

6.2.3 The regression

The relative sea-level curve from the Tasiusaq area indicates a rapid regression from 26 m a.h.a.t. to present day sea level in about 700 years (8750 to 8050 cal. yr BP), corresponding to almost 4 cm year^{-1}. Up till then the relative sea level must already have fallen about 14 m from the highest marine limit in Tasiusaq. In the Qaqortoq area, the regression was somewhat slower, 25 m between 10 000 and 8800 cal. yr BP, corresponding to *c.* 2 cm year^{-1} (Sparrenbom *et al.* 2006b). The relative sea level in the Tasiusaq area continued to fall, but at a much slower rate, and reached below 3.5 m b.h.a.t. at 7300 cal. yr BP.

According to the compilation in Figure 20, the regression started earlier in Nanortalik than Qaqortoq and later in Tasiusaq. This is a result of the northeastwards retreating ice sheet into the fjords. Figure 20 shows that the "visible" part of the regression in Tasiusaq was about 1000 year later than in Qaqortoq and 2000 years later than in Nanortalik.

Shorelines of different ages have been compared in Figure 21. When the shoreline was situated at 26 m a.h.a.t. in the Tasiusaq area at about 8750 cal. yr BP (Randsalu 2008), most of the regression in Nanortalik and Qaqortoq was almost completed.

More complicated are the basins K1 and K3 (Fig. 20) situated between Tasiusaq and Qaqortoq. They indicate an earlier regression than in Qaqortoq. This may imply that the area between Qaqortoq and Tasiusaq had lost more ice than the coastal areas and the inner fjord areas. Another possible explanation or additional factor could be complexities related to the collapse of the Laurentide peripheral bulge.

The old Nu1 age from the study area (Sparrenbom *et al.* 2006b) does not concur with the other sea-level data points. If the age is correct, the only plausible explanation is that the threshold must have been substantially higher due to, for example, damming of ice remaining in the narrow strait were the lake is drained into the fjord. However, the estimated marine limit from Tasiusaq is still much younger, which puts doubts on the Nu1 ^{14}C ages.

6.2.4 The lower sea-level limit

The Holocene climatic optimum in Greenland have been dated to between 8000 and 5000 yr BP (Dahl-Jensen 1998, Andresen *et al.* 2004) and to between 6000 and 3000 cal. yr BP (Kaplan *et al.* 2002). The ice sheet during this period had retreated behind its present position (Weidick 2004), perhaps as much as 30 km (Sparrenbom *et al.* 2006d).

The investigated marine embayment (Ta4) in this study suggests that the relative sea level in the

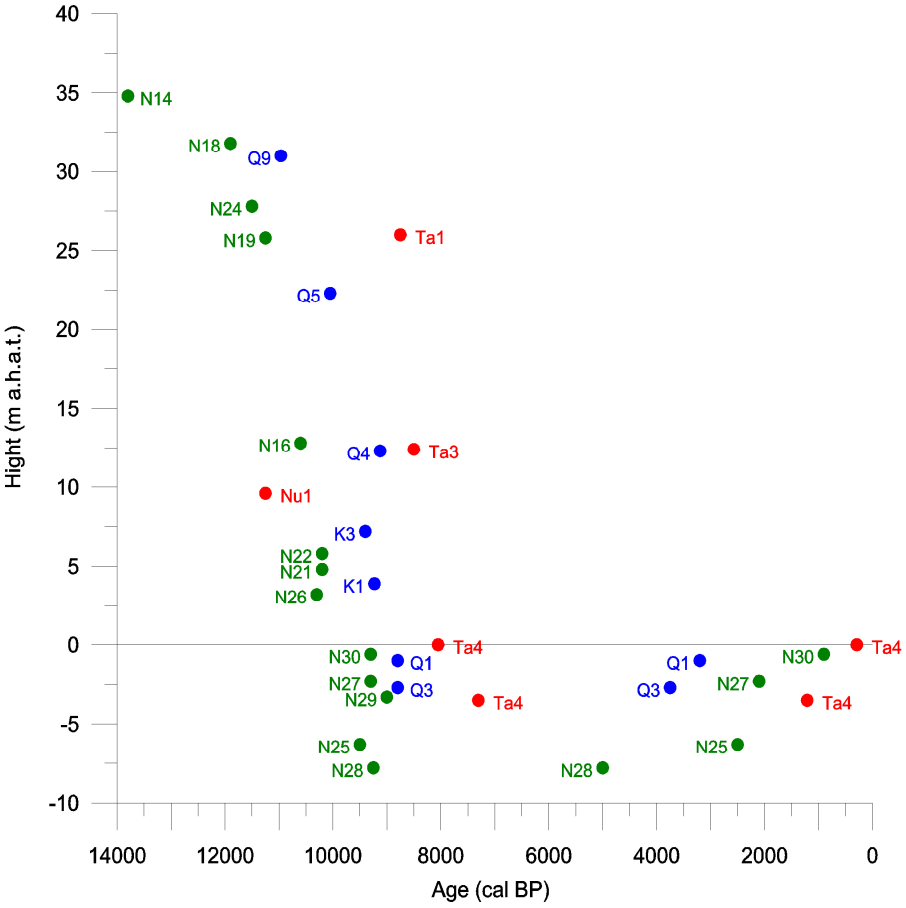

Figure 20. A simplified compilation of selected sea-level data from the Julianehåb area. Red dots are from the Tasiusaq area, Ta1 and Ta3 from Randsalu (2008), Ta4 from this study and Nu1 from Sparrenbom *et al.* (2006b). Blue dots are from the Quaqortoq area (Sparrenbom *et al.* 2006b). Green dots are from the Nanortalik area (Bennike *et al.* 2002, Sparren-bom *et al.* 2006a). Error bars are excluded from this compilation.

Tasiusaq area stayed below present sea level between 8050 and 290 cal. yr BP. The study also suggests that the relative sea level stayed below 3.5 m b.h.a.t. between 7300 and 1210 cal. yr BP. How much further down the regression continued is more difficult to estimate. The drowned beach at Qassiarsuk is situated at *c.* 4-5 m b.h.a.t. (Kuijpers *et al.* 1999). An isolation sequence in another cored marine basin in the study area (Nu2, Table 4), with a threshold situated at approximately 4.5 m b.h.a.t. has been found (Bennike, personal communication). This shows that the relative sea level reached below 4.5 m b.h.a.t. during some part of the Holocene. In Narsaq a dry crust was found at *c.* 10 m b.h.a.t., but is situated 25 km southwest of the study area. All in all, sea level reached lower than 4.5 m b.h.a.t., but probably not more than 10 m b.h.a.t. Whether this low-stand occurred during a longer or a shorter period before it started to rise again is not known. The climate optimum lasted about 3000 years, suggesting that the ice sheet might have stayed at a minimum extent during at least a few millennia. More investigations of basins situated below present sea level are needed to more accurately show how low, and for how long time, the relative sea level reached its minimum in the Tasiusaq area.

6.2.5 The Neoglaciation

Cooler conditions have been recorded at *c.* 3700 cal. yr BP (Andresen *et al.* 2004) and at *c.* 3000 cal. yr BP (Kaplan *et al.* 2002). The only dating of material in moraines by Kelly (1975) suggests that the expansion of the ice sheet did not start before *c.* 5300 cal. yr BP. The start of the neoglaciation have been estimated by Weidick *et al.* (2004) to *c.* 3000-4000 cal. yr BP and modelling by Sparrenbom *et al.* (2006d) suggests a start at *c.* 6500 yr BP. The first sign of a neoglaciation from the Tasiusaq area is the transgression sequence dated to 1210 cal. yr BP. The glacial expansion could, however, have been going on for some time before the lithosphere responded by being pressed down and before sea level reached 3.5 m b.h.a.t.

6.2.6 The transgression

The fist sign of a transgression in the studied basin (Ta4) with a threshold at 3.5 m b.h.a.t. is dated to 1210 cal. yr BP. The time when the present day level was reached has been dated to 290 cal. yr BP, but there is some uncertainty with this age. This transgression seems to have occurred fairly rapid, with a 3.5 m sea level rise in about 900 years, corresponding to *c.* 4 mm per year. In Nanortalik the transgression pace has been estimated to 1.5 to 2 mm per year (Sparrenbom *et al.* 2006a) and 3 mm per year in Qaqortoq (Sparrenbom *et al.* 2006b). It is also noteworthy that the transgression probably occurred more than 2000 years earlier in Nanortalik and Qaqortoq than in Tasiusaq.

The obvious explanation for a late Holocene transgression in southern Greenland is the neoglacial

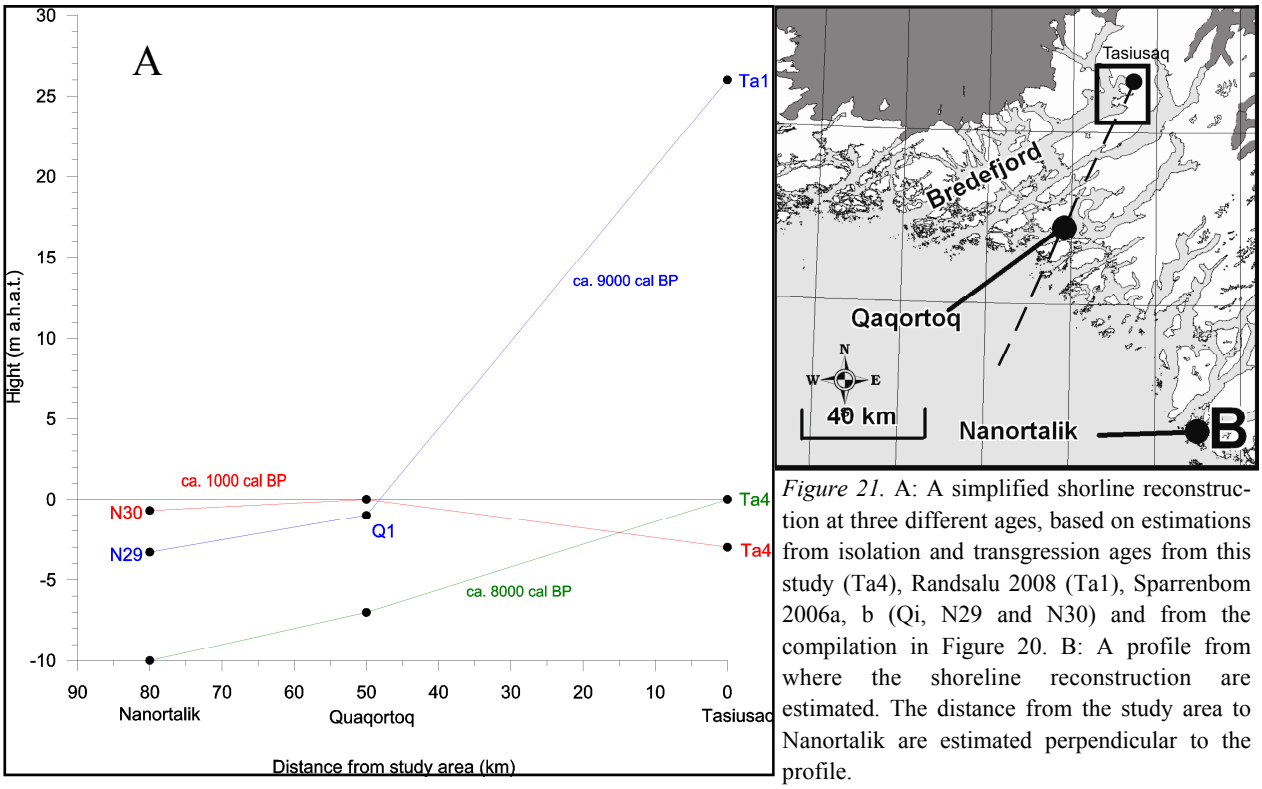

Figure 21. A: A simplified shorline reconstruction at three different ages, based on estimations from isolation and transgression ages from this study (Ta4), Randsalu 2008 (Ta1), Sparrenbom 2006a, b (Qi, N29 and N30) and from the compilation in Figure 20. B: A profile from where the shoreline reconstruction are estimated. The distance from the study area to Nanortalik are estimated perpendicular to the profile.

advance pressing down the lithosphere. The ice equivalent sea level has, since 7000 cal. yr BP, only risen at the most a few metres (Fleming *et al.* 1998). If a glacial advance was the only cause, the transgression should logically start earlier in the Tasiusaq area than in Nanortalik and Qaqortoq, as Tasiusaq is situated closer to the ice sheet. This does not seem to be the case. Also, the shoreline reconstruction (Fig. 21) and the relative sea-level curve (Fig. 20) indicate that the relative sea-level rise started earlier in Nanortalik and Qaqortoq, suggesting that there are different components causing the transgression registered in the Julianehåb district.

A possible explanation for an earlier transgression in Qaqortoq and Nanortalik than in Tasiusaq, is that the outer coast was more affected by the collapse of the peripheral bulge of the huge and late deglaciated Laurentide Ice Sheet. This could have happened at about 4000-5000 cal. yr BP when the first transgression is recorded (Sparrenbom *et al.* 2006a, b). The transgression in Tasiusaq could instead be the result of the neoglaciation that occurred a couple of thousands year later and also caused a more rapid sea-level rise. An ice sheet advance, named the Narssarssuaq stade, is dated to about 2000 cal. yr BP (Bennike & Sparrenbom 2007), but was probably too small to alone affect sea level markedly. A more far-fetched hypothesis is if the ice sheet expansion happened earlier in the mountains that surround the Julianehåb area, affecting the Nanortalik and Qaqortoq region before the Tasiusaq area.

A relative sea-level rise during the last thousand years in the Tasiusaq area explains the more or less submerged ruins from the Norse time.

More data from submarine basins in the Bredefjord area are needed to understand the timing of the late Holocene transgression in Tasiusaq and the affects from the neoglaciation readvance and the collapse of the Laurentide peripheral bulge in the Julianehåb district.

7 Conclusions

1. The southern part of the Greenland Ice Sheet retreated from the Tasiusaq area sometime before 9000 cal. yr BP as a response to the warmer climate.

2. The marine limit in Tasiusaq area is about 40 m a.h.a.t. and is similar (± 10 m) over the whole Julianehåb district. Comparisons of the marine limit in the area suggest that much of the uplift occurred before the Tasiusaq area was finally deglaciated.

3. A rapid regression from 26.0 to 0.0 m a.h.a.t. occurred in the Tasiusaq area between about 8750 and 8050 cal. yr BP (4 cm per year). The regression happened about 1000 years earlier in Qaqortoq and about 2000 years earlier in Nanortalik as a consequence of earlier deglaciation in the latter areas.

4. The relative sea level fell below present day level at about 8050 cal. yr BP in the Tasiusaq area. The relative sea level continued to fall and reached below 3.5 m b.h.a.t. at 7300 cal. yr BP.

5. The lowest relative sea level in the Tasiusaq area was somewhere between 4.5 and 10 m b.h.a.t., and was reached sometime between 7000 and 3000 cal. yr BP.

6. Two units in the Ta4 sediment sequence may record increased erosion, suggesting wetter climate around 3400 and 1750 cal. yr BP.

7. The neoglacial readvance was probably responsible for the transgression in the Tasiusaq area that started sometime before 1210 cal. yr BP, when the relative sea level reached 3.5 m b.h.a.t. The relative sea level continued to rise and reached present day level sometime during the last 500 years. The transgression started more than 2000 years earlier in Qaqortoq and Nanortalik. This anomaly may be explained by differential effects from the collapse of the Laurentide Ice Sheet peripheral bulge and the neoglacial readvance, between the coastal areas of Nanortalik and Qaqortoq and the inner Bredefjord area. Another possibility is a different ice sheet configuration than the one modelled by Sparrenbom *et al.* (2006d).

8. This investigation has shown that the Julianehåb district has a complex sea-level history. More sea level data from this area are needed to better understand the timing and effects from the neoglaciation and the Laurentide peripheral bulge.

8 Acknowledgements

First and most I want to thank my supervisors Charlotte Sparrenbom, Svante Björck, Ole Bennike and Kurt Lambeck. Thank you Charlotte, for always being available for discussions of all possible issues and for constantly giving new ideas to improve this work. I am very grateful for your support throughout this project, especially during fieldwork and macrofossil analysis. I owe great debt to Svante, for being available to answer and discuss all my questions. Thank you for inspiring me to apply new ideas and thoughts to my writing. All time spend reading my manuscript during the last few weeks by Charlotte and Svante is highly appreciated. Thank you Ole, for all help with the macrofossil analysis, discussions during fieldwork and for teaching me all secrets regarding lake coring. Thank you Kurt, for inspiring discussions and for support during fieldwork. I also want to Thank Dan Zwarts for assistance in field, especially for the tide and GPS measurements. Karl Ljung is acknowledged for discussions regarding XRF-scanning and Pia Sköld for discussions regarding radiocarbon dating. I also want to thank Linda Randsalu for good cooperation and for fruitful discussions throughout this project. The Australian Research Council, the Australian National University and the Swedish Polar Secreteriat is acknowledged for the founding and logistic support. Finally I want to thank all teachers and students I have meet during my years at the geology department who made it to such a pleasant time.

9 References

Andresen C.S., Björck, S., Bennike, O. & Bond, G., 2004: Holocene climate changes in southern Greenland: evidence from lake sediments. *Journal of Quaternary Science 19, 8*, 783-795.

Bennike, O. & Björck, S., 2002: Chronology of the last recession of the Greenland Ice Sheet. *Journal of Quaternary Science 17, 3,* 211-219.

Bennike, O., Björck, S. & Lambeck, K., 2002: Estimates of South Greenland late-glacial ice limits from a new relative sea level curve. *Earth and Planetary Science Letters 197*, 171-186.

Bennike, O. & Sparrenbom C.J., 2007: Dating of the Narssarssuaq stade in southern Greenland. *The Holocene 17, 2*, 279-282.

Böcher, J., Knudsen, J., Larsen, S. & Vilhelmsen, L., 2001: *Insekter og andre smådyr – i Grønlands fjeld og ferskvand.* Copenhagen.

Böning, P., Bard, E. & Rose, J., 2007: Toward direct, micron-scale XRF elemental maps and quantitative profiles of wet marine sediments. *Geochemistry. Geophysics. Geosystems. 8*, 1-14

Cappelen, J., Jørgensen, B.V., Laursen, E.V., Stannius, L.S. & Thomsen, R.S., 2001: The observed climate of Greenland, 1958-99 - with climatological standard normals, 1961-90. *Danish Meteorological Institute, Technical Report 00-18*, 154 pp.

Dahl-Jensen, D., Mosegaard, K., Gundestrup, N., Clow, G.D., Johnsen, S.J., Hansen, A.W. & Balling, N., 1998: Past Temperatures Directly from the Greenland Ice Sheet. *Science 282*, 268-271.

Daryin A.V., Kalugin, I.A., Maksimova, N.V., Smolyaninova L.G. & Zolotarev, K.V., 2005: Use of a scanning XRF analysis on SR beams from VEPP-3 storage ring for research of core bottom sediments from Teletskoe Lake with the purpose of high resolution quantitative reconstruction of last millennium paleoclimate. *Nuclear Instruments and Methods in Physics Research A 543*, 255-258.

Dean, W., 1974: Determination of carbonate and organic matter in calcareous sediments and sedimentary rocks by loss on ignition: comparison with other methods. *Journal of Sedimentary Petrology 44*, 242-248.

Farvandsvæsenet, 2006: *Tidevandstabeller 2007 for Grønlandske Farvande*. Farvandsvæsenet, Copenhagen.

Fleming, K., Johnston, P., Zwartz, D., Yokoyama, Y., Lambeck, K. & Chappell, J., 1998: Refining the eustatic sea-level curve since the Last Glacial Maximum using far- and intermediate-field sites. *Earth and Planetary Science Letters 163*, 327-342.

Fleming, K. & Lambeck, K., 2004: Constraints on the Greenland Ice Sheet since the Last Glacial Maximum from sea-level observations and glacial-rebound models. *Quaternary Science Reviews 23*, 1053-1077.

Foersom, T., Kapel, F. & Svarre, O., 1997: *Grønlands flora i farver*. Nuuk.

Fredskild, B., 1973: Studies in the vegetational history of Greenland, paleobotanical investigations of some Holocene lake and bog deposits. *Meddelelser om Grønland 198, 4, 245 pp.*

Funder, S., 1979: The Quaternary geology of the Narssaq area, South Greenland. *Grønlands Geologiske Undersøgelse, Rapport 86*, 24 pp.

Gabel-Jørgensen, C.C.A., Egedal, J., 1940: Tidal observations made at Nanortalik and Julianehåb in 1932-1934. *Meddelelser om Grønland 107, 2*, 1-47.

Heiri, O., Lotter, A.F. & Lemcke, G., 2001: Loss on ignition as a method for estimating organic and carbonate content in sediments: reproducibility and comparability of results. *Journal of Paleolimnology 25*, 101-110.

Hughen, K.A., Baillie, M.G.L., Bard, E., Beck, J.W., Bertrand, C.J.H., Blackwell, P.G., Buck, C.E., Burr, G.S., Cutler, K.B., Damon, P.E., Edwards, R.L., Fairbanks, R.G., Friedrich, M., Guilderson, T.P., Kromer, B., McCormac, G., Manning, S., Ramsey, C.B., Reimer, P.J., Reimer, R.W., Remmele, S., Southon, J.R., Stuiver, M., Talamo, S., Taylor, F.W., van der Plicht, J. & Weyhenmeyer, C.E., 2004: Marine04 Marine Radiocarbon Age Calibration, 0–26 Cal Kyr BP, *Radiocarbon 46, 3*, 1059-1086.

Jensen, K.G., Kuijpers, A., Koç, N. & Heinemeier, J., 2004: Diatom evidence of hydrographic changes and ice conditions in Igaliku Fjord, South Greenland, during the past 1500 years. *The Holocene 14, 2,* 152-164.

Kaplan, M.R., Wolfe, A.P. & Miller, G.H., 2002: Holocene Environmental Variability in Southern Greenland Inferred from Lake Sediments. *Quaternary Research 58*, 149-159.

Kelly, M., 1975: A note on the implications of two radiocarbon dated samples from Qaleragdlit imâ, South Greenland. *Bulletin of the Geological Society of Denmark 24,* 21-26.

Kelly, M., 1980: The status of the Neoglacial in western Greenland. *Grønlands geologiske undersøkelse, Rapport 96*. 24 pp.

Kuijpers, A., Abrahamsen, N., Hoffman, G., Hühnerbach, V., Konradi, P., Kunzendorf., Mikkelsen, N., Thiede, J., Wilhelm, W., & shipboard scientific party of RV Poseidon, and surveyors of the Royal Danish Administration for Navigation and Hydrography., 1999: Climate change and the Viking-age fjord environment of the Eastern Settlement, South Greenland. *Geology of Greenland Survey. Bulletin 183*, 61-67.

Lambeck K., 2001: Sea Level Change Through the Last Glacial Cycle. *Science 292*, 679-686.

Lassen, S.J., Kuijpers, A., Kunzendorf, H., Hoffman-Wieck, G., Mikkelsen, N. & Konradi, P., 2004: Late-Holocene Atlantic bottom-water variability in Igaliku Fjord, South Greenland, reconstructed from foraminifera faunas. *The Holocene 14, 2*, 165-171.

Ljung, K. & Björck, S, 2004: A lacustrine record of the Pleistocene-Holocene boundary in southernmost Greenland. *GFF 126*, 273-278.

Mathiassen, T., 1936. The Eskimo archaeology of Julianehaab district. *Meddelelser om Grønland 118, 1,* 1-141.

Moreno, A., Giralt, S., Valero-Garcés, A., Sáez, A., Bao, R., Prego, R., Pueyo, J.J., González-Sampériz, P. & Taberner, C., 2007: A 14 kyr record of the tropical Andes: The Lago Chungará sequence (18° S, northern Chilean Altiplano). *Quaternary International 161*, 4-21.

Nilsson, T., 1961: Kvartärpaleontologi. Lund.

Randsalu, L., 2008: Post glacial relative sea-level changes in the Tasiusaq area, southwest Greenland. *Examensarbeten i geologi vid Lunds Universitet - Kvartärgeologi, nr. 220.*

Reimer, P.J., Baillie, M.G.L., Bard, E., Bayliss, A., Beck, J.W., Bertrand, C.J.H., Blackwell P.G., Buck, C.E., Burr, G.S., Cutler, K.B., Damon, P.E., Edwards, R.L., Fairbanks, R.G., Friedrich, M., Guilderson, T.P., Hogg, A.G., Hughen, K.A., Kromer, B., McCormac, G., Manning, S., Stuiver, M., Talamo, S., Taylor, F.W., van der Plicht, J. & Weyhenmeyer, C.E., 2004: IntCal04 Terrestrial radiocarbon age calibration, 0-26 cal kyr BP. *Radiocarbon 46*, 1029-1058.

Rueness, J., 1977: *Norsk algeflora*. Universitetsforlaget Oslo, Bergen, Tromsø.

Shotton, F.W., Williams, R.E.G., Johnson, A.S., 1974: *Radiocarbon 16*, 285-303.

Sparrenbom C.J., Bennike, O., Björck, S. & Lambeck, K., 2006a: Relative sea-level changes since 15 000 cal yr. BP in the Nanortalik area, southern Greenland. *Journal of Quaternary Science 21, 1*, 29-48.

Sparrenbom C.J., Bennike, O., Björck, S. & Lambeck, K., 2006b: Holocene relative sea-level changes in the Qaqortoq area, southern Greenland. *Boreas 35*, 171-187.

Sparrenbom C.J., Rindby, A. & Kortekaas, M., 2006c: XRF-scanning, an effective method in the search for changing sea levels recorded as isolation contacts/ transgression sequences. *In Sparrenbom C.J.: Constraining the southern part of the Greenland Ice Sheet since the Last Glacial Maximum from relative sea-level changes, cosmogenic dates and glacial-isostatic adjustments models, Appendix 3.* Lundqua Thesis 56, Lund.

Sparrenbom C.J., Lambeck, K., Fabel, D., Fleming, K. & Purcell, A., 2006d: Constraining the southern Greenland Ice Sheet since the Last Glacial Maximum from sea-level observations, cosmogenic dates and glacial-isostatic adjustment models. *In Sparrenbom C.J.: Constraining the southern part of the Greenland Ice Sheet since the Last Glacial Maximum from relative sea-level changes, cosmogenic dates and glacial-isostatic adjustments models, Appendix 4.* Lundqua Thesis 56, Lund.

Sørensen, H., Andersen, T., Emeleus, C.H., Secher, K., Upton, B.G.J. & Weidick, A., 2006: *Geological guide, south Greenland, The Narsarsuaq - Narsaq - Qaqortoq region.* Geological survey of Denmark and Greenland. Copenhagen.

Tarasov, L & Peltier, W.R., 2002: Greenland glacial history and local geodynamic consequences. *Geophysical Journal of International 150*, 198-229.

Weidick, A., 1975: Quaternary geology of the area between Fredrikshåbs Isblink and Ameralik. *Rapport Grønlands geologiske undersøkelse 70*, 22pp.

Weidick, A., 1984: Studies of Glacier Behaviour and Glacier Mass Balance in Greenland: A Review. *Geografiska Annaler 66A, 3*, 183-195.

Weidick, A., 1987: Quaternary map of Greenland, sheet 1, Sydgrønland. 1:500,000. Geodætisk Institut, Denmark.

Weidick, A., Kelly, M. & Bennike, O., 2004: Late Quaternary development of the southern sector of the Greenland Ice Sheet, with particular reference to the Qassimiut lobe. *Boreas 33, 4,* 284-299.

Appendix 1. All XRF-scanned elements in the Ta4 sediment sequence

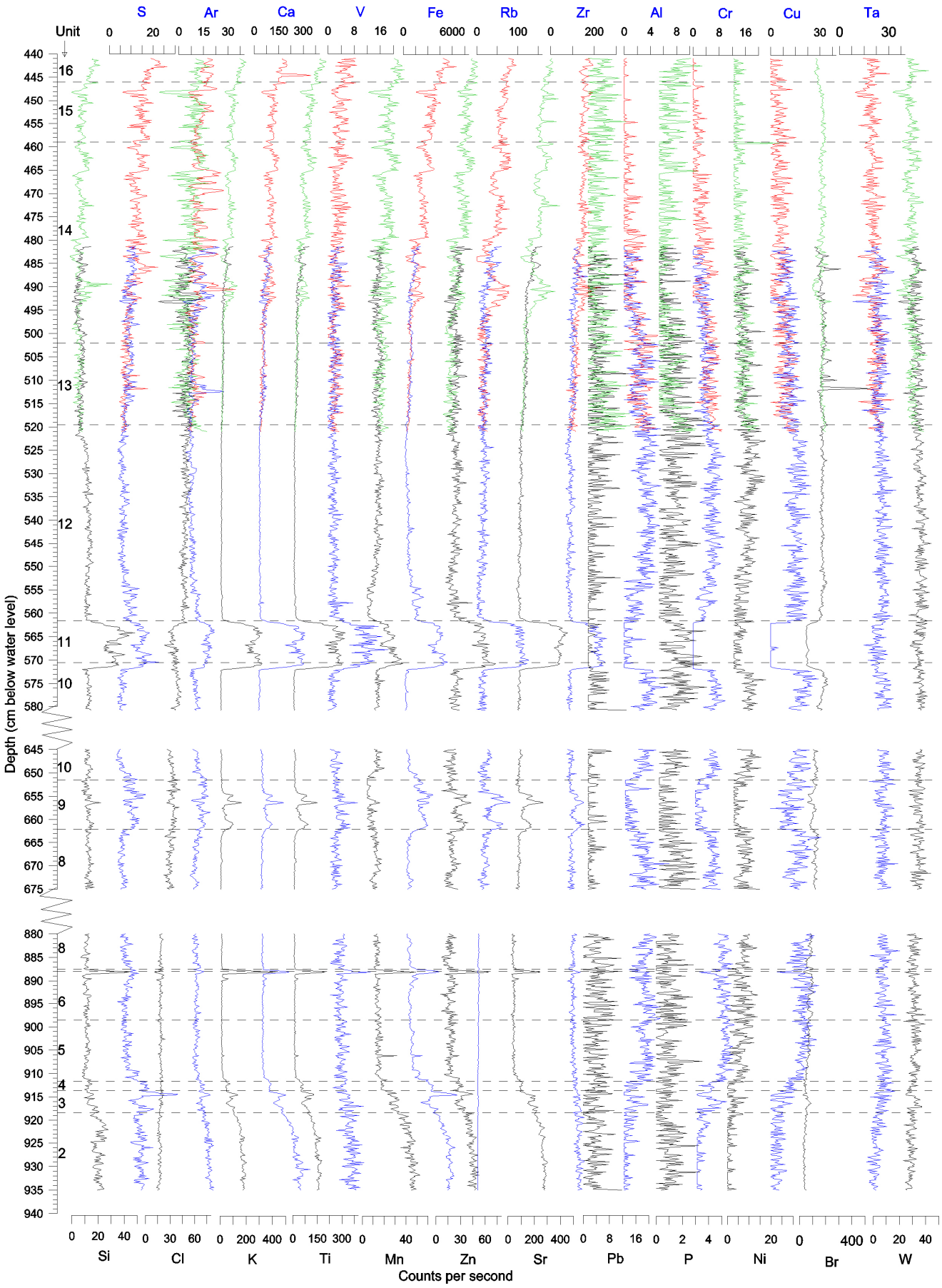

Appendix 2a - Marine macrofossil

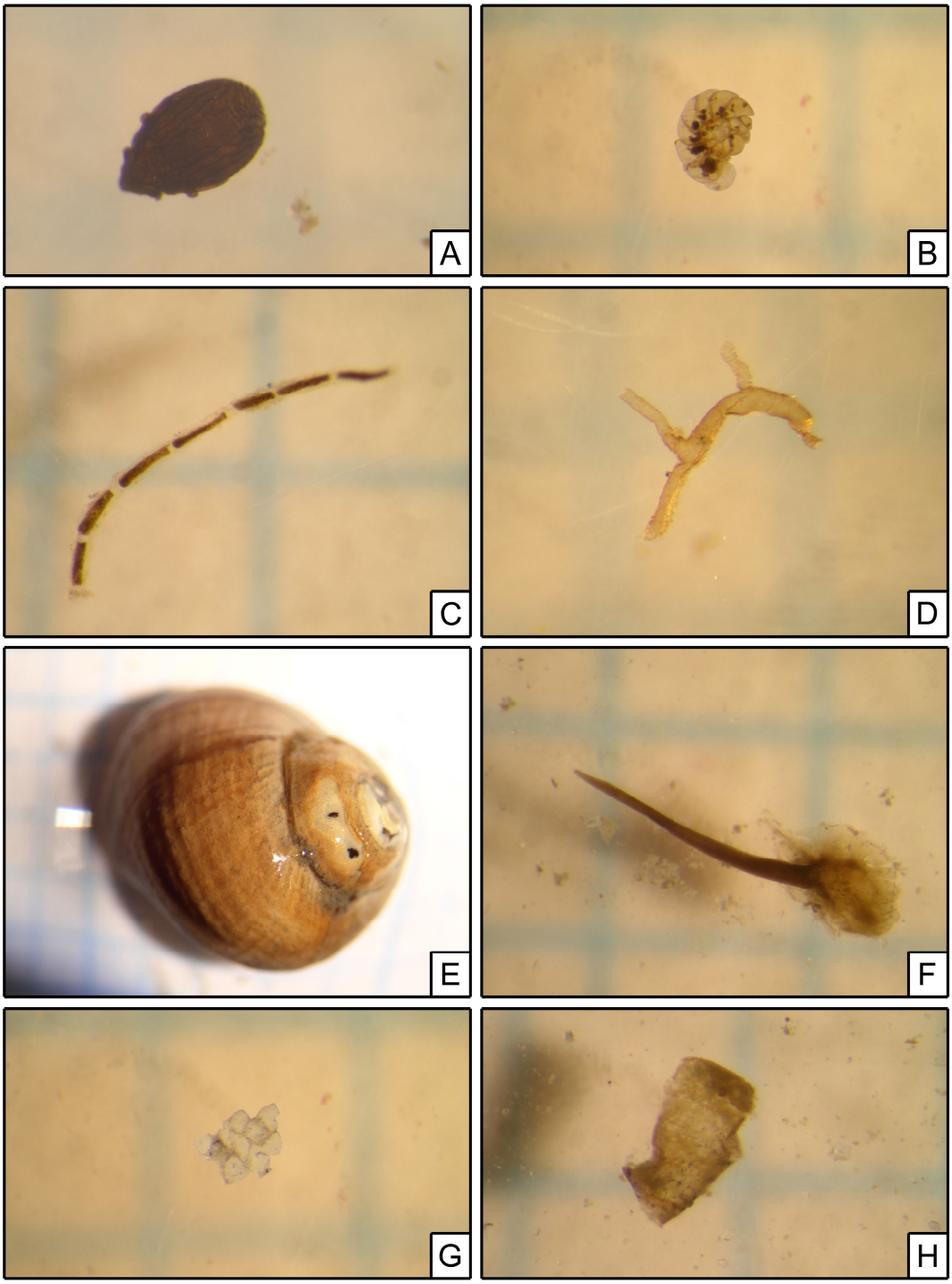

A. *Ameronothrus sp.*
B. Foraminifera indet.
C. *Goniotrichum sp.*
D. Hydroidea indet.
E. *Littorina sp.*
F. *Mytilus edulis*
G. *Pectinaria sp.*
H. Phaeophyceae indet.

Scale: 1 mm between the bluelines in the background.

Appendix 2b - Marine and brackish macrofossil

Marine

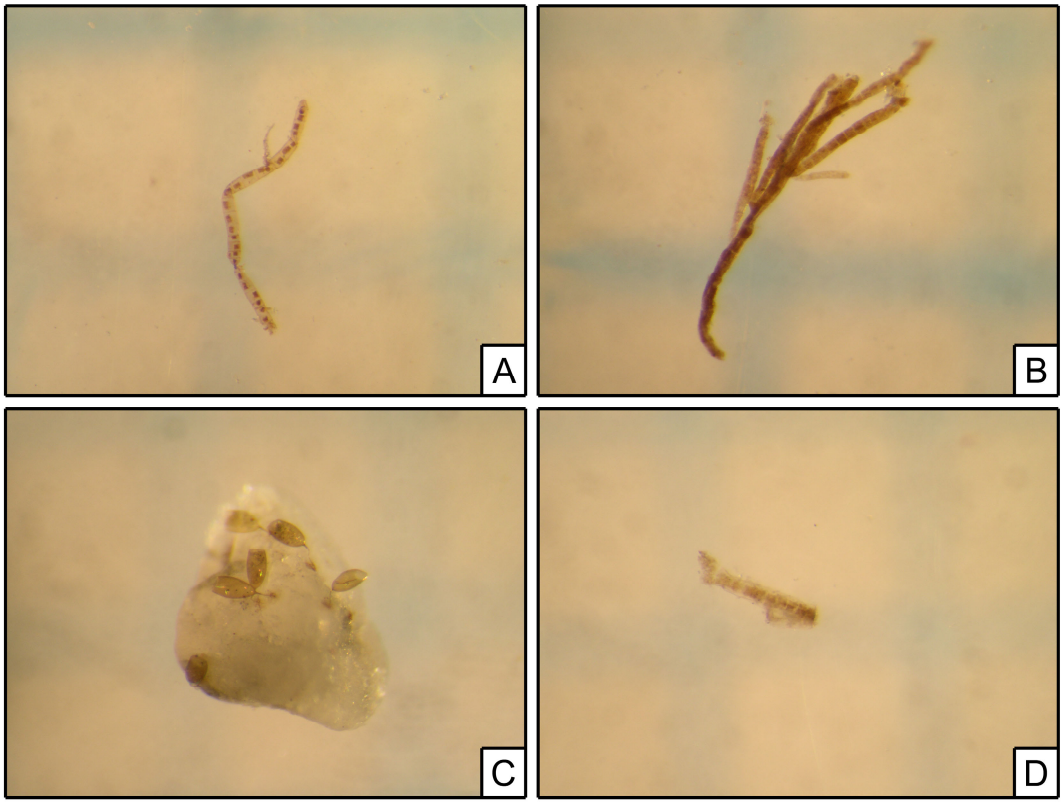

Brackish

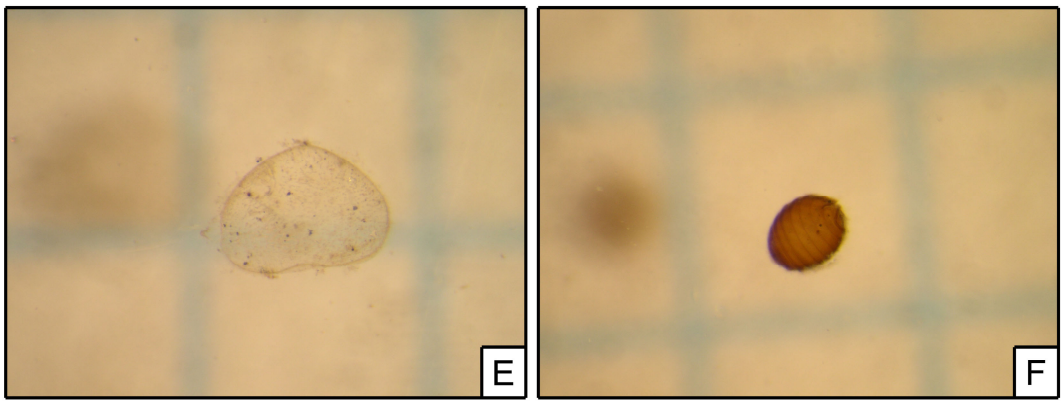

A. *Rhizoclonium sp.*
B. *Sphacelaria sp.*
C. Tricladida indet.
D. *Ulothrix sp.*
E. *Sarscypridopsis aculeata*
F. *Tolypella sp.*

Scale: 1 mm between the bluelines in the background.

Appendix 2c - Lacustrine macrofossil

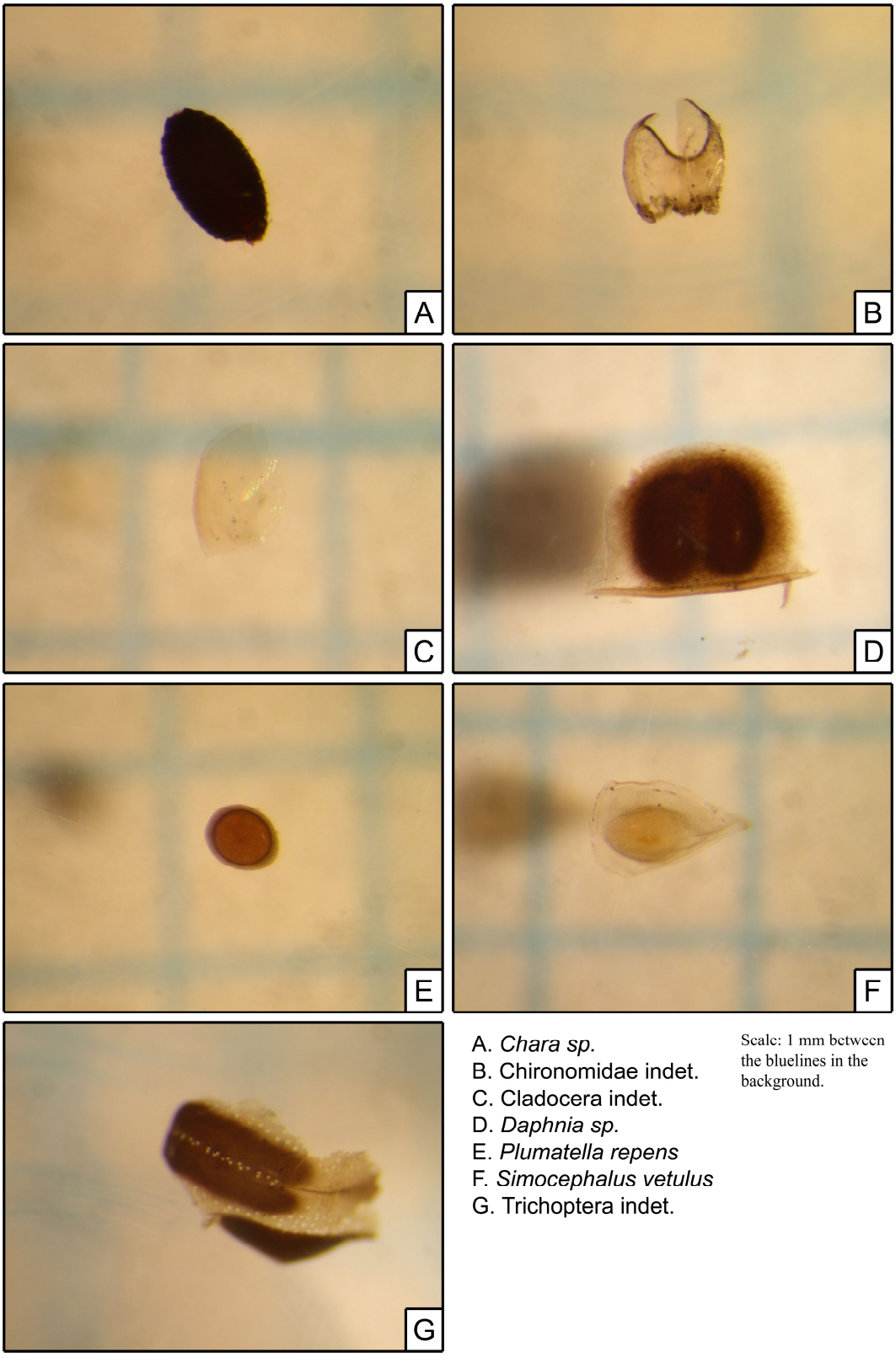

A. *Chara sp.*
B. Chironomidae indet.
C. Cladocera indet.
D. *Daphnia sp.*
E. *Plumatella repens*
F. *Simocephalus vetulus*
G. Trichoptera indet.

Scale: 1 mm between the bluelines in the background.

Appendix 2d - Terrestrial macrofossil

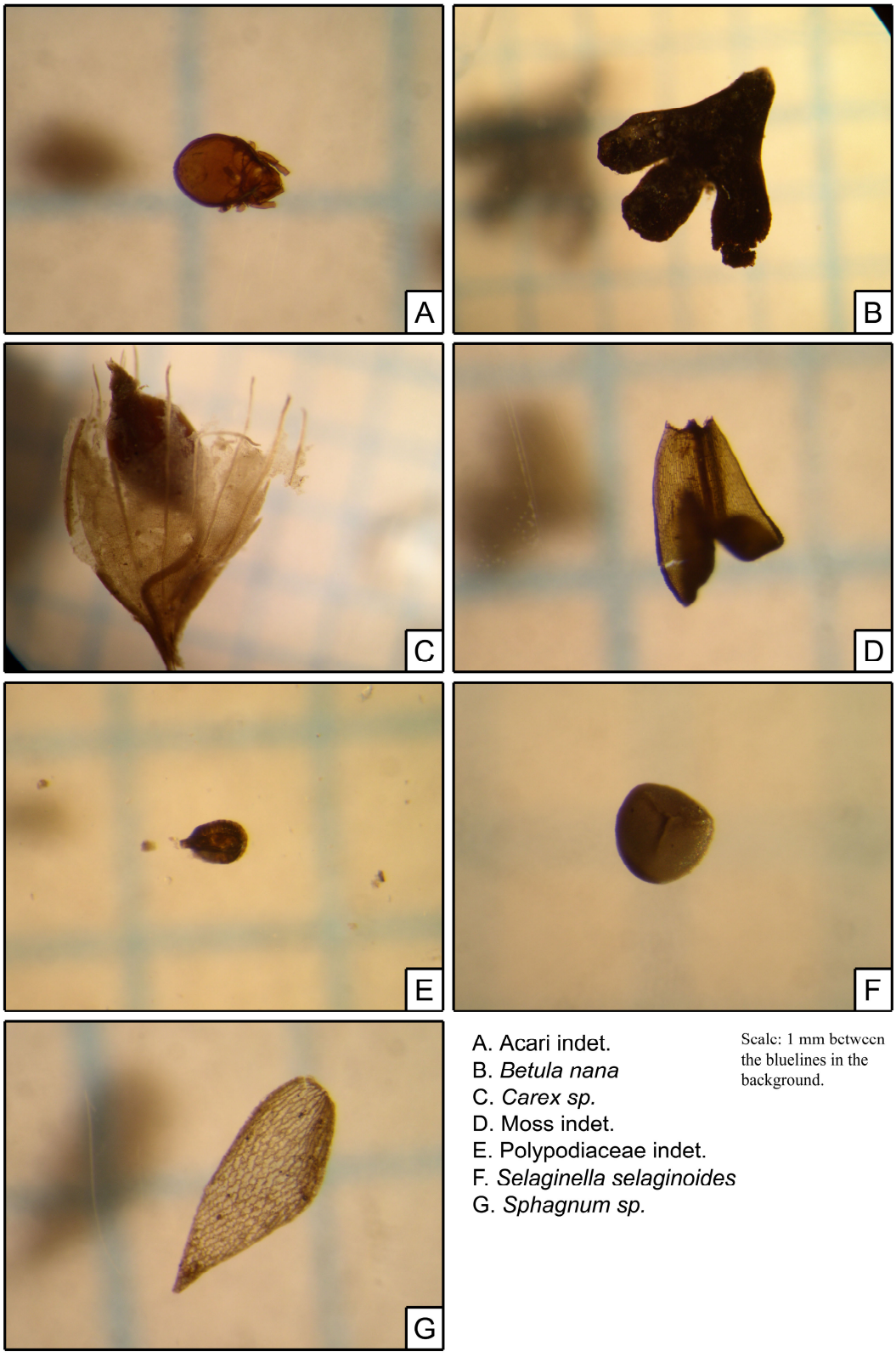

A. Acari indet.
B. *Betula nana*
C. *Carex sp.*
D. Moss indet.
E. Polypodiaceae indet.
F. *Selaginella selaginoides*
G. *Sphagnum sp.*

Scale: 1 mm between the bluelines in the background.

Tidigare skrifter i serien "Examensarbeten i Geologi vid Lunds Universitet":

174. Jonsson, Sara, 2004: Structural control of fine-grained granite dykes at the Äspö Hard Rock Laboratory, north of Oskarshamn, Sweden.
175. Ljungberg, Carina, 2004: Belemniters stabila isotopsammansättning: paleomiljöns och diagenesens betydelse.
176. Oster, Jessica, 2004: A stratigraphic study of a coastal section through a Late Weichselian kettle hole basin at Ålabodarna, western Skåne, Sweden.
177. Einarsson, Elisabeth, 2004: Morphological and functional differences between rhamphorhynchoid and pterodactyloid pterosaurs with emphasis on flight.
178. Anell, Ingrid, 2004: Subsidence in rift zones; Analyzing results from repeated precision leveling of the Vogar Profile on the Reykjanes Peninsula, Southwest Iceland.
179. Wall, Torbjörn, 2004: Magnetic grain-size analyses of Holocene sediments in the North Atlantic and Norwegian Sea – palaeoceano-graphic applications.
180. Mellgren, Johanna, S., 2005: A model of reconstruction for the oral apparatus of the Ordovician conodont genus *Protopanderodus* Lindström, 1971.
181. Jansson, Cecilia, 2005: Krossbergskvalitet och petrografi i den kambriska Hardebergasandstenen i Skåne.
182. Öst, Jan-Olof, 2005: En övergripande beskrivning av malmbildande processer med detaljstudier av en bandad järnmalm från södra Dalarna, Bergslagen.
183. Bragée, Petra, 2005: A palaeoecological study of Holocene lake sediments above the highest shoreline in the province of Västerbotten, northeast Sweden.
184. Larsson, Peter, 2005: Palynofacies och mineralogi över krita-paleogengränsen vid Stevns Klint och Kjølby Gaard, Danmark.
185. Åberg, Lina, 2005: Metamorphic study of metasediment from the Kangilinaaq Peninsula, West Greenland.
186. Sidgren, Ann-Sofie, 2005: $^{40}Ar/^{39}Ar$-geokronologi i det Rinkiska bältet, västra Grönland.
187. Gustavsson, Lena, 2005: The Late Silurian Lau Event and brachiopods from Gotland, Sweden.
188. Nilsson, Eva K., 2005: Extinctions and faunal turnovers of early vertebrates during the Late Silurian Lau Event, Gotland, Sweden.
189. Czarniecka, Ursula, 2005: Investigations of infiltration basins at the Vomb Water Plant – a study of possible causes of reduced infiltration capacity.
190. G³owacka, Ma³gorzata, 2005: Soil and groundwater contamination with gasoline and diesel oil. Assessment of subsurface hydrocarbon contamination resulting from a fuel release from an underground storage tank in Vanstad, Skåne, Sweden.
191. Wennerberg, Hans, 2005: A study of early Holocene climate changes in Småland, Sweden, with focus on the '8.2 kyr event'.
192. Nolvi, Maria & Thorelli, Gunilla, 2006: Extraterrestrisk och terrestrisk kromrik spinell i fanerozoiska kondenserade sediment.
193. Nilsson, Andreas, 2006: Palaeomagnetic secular variations in the varved sediments of Lake Goœci¹¿, Poland: testing the stability of the natural remanent magnetization and validity of relative palaeointensity estimates.
194. Nilsson, Anders, 2006: Limnological responses to late Holocene permafrost dynamics at the Stordalen mire, Abisko, northern Sweden.
195. Nilsson, Susanne, 2006: Sedimentary facies and fauna of the Late Silurian Bjärsjölagård Limestone Member (Klinta Formation), Skåne, Sweden.
196. Sköld, Eva, 2006: Kulturlandskapets förändringar inom röjningsröseområdet Yttra Berg, Halland - en pollenanalytisk undersökning av de senaste 5000 åren.
197. Göransson, Ammy, 2006: Lokala miljöförändringar i samband med en plötslig havsyteförändring ca 8200 år före nutid vid Kalvöviken i centrala Blekinge.
198. Brunzell, Anna, 2006: Geofysiska mätningar och visualisering för bedömning av heterogeniteters utbredning i en isälvsavlagring med betydelse för grundvattenflöde.
199. Erlfeldt, Åsa, 2006: Brachiopod faunal dynamics during the Silurian Ireviken Event, Gotland, Sweden.

200. Vollert, Victoria, 2006: Petrografisk och geokemisk karaktärisering av metabasiter i Herrestadsområdet, Småland.
201. Rasmussen, Karin, 2006: En provenansstudie av Kågerödformationen i NV Skåne – tungmineral och petrografi.
202. Karlsson, Jonnina, P., 2006: An investigation of the Felsic Ramiane Pluton, in the Monapo Structure, Northern Moçambique.
203. Jansson, Ida-Maria, 2006: An Early Jurassic conifer-dominated assemblage of the Clarence-Moreton Basin, eastern Australia.
204. Striberger, Johan, 2006: En lito- och biostratigrafisk studie av senglaciala sediment från Skuremåla, Blekinge.
205. Bergelin, Ingemar, 2006: $^{40}Ar/^{39}Ar$ geochronology of basalts in Scania, S Sweden: evidence for two pulses at 191-178 Ma and 110 Ma, and their relation to the breakup of Pangea.
206. Edvarssson, Johannes, 2006: Dendrokronologisk undersökning av tallbestånds etablering, tillväxtdynamik och degenerering orsakat av klimatrelaterade hydrologiska variationer på Viss mosse och Åbuamossen, Skåne, södra Sverige, 7300-3200 cal. BP.
207. Stenfeldt, Fredrik, 2006: Litostratigrafiska studier av en platåformad sand- och grusavlagring i Skuremåla, Blekinge.
208. Dahlenborg, Lars, 2007: A Rock Magnetic Study of the Åkerberg Gold Deposit, Northern Sweden.
209. Olsson, Johan, 2007: Två svekofenniska graniter i Bottniska bassängen; utbredning, U-Pb zirkondatering och test av olika abrasionstekniker.
210. Erlandsson, Maria, 2007: Den geologiska utvecklingen av västra Hamrångesynklinalens suprakrustalbergarter, centrala Sverige.
211. Nilsson, Pernilla, 2007: Kvidingedeltat – bildningsprocesser och arkitektonisk uppbyggnadsmodell av ett glacifluvialt Gilbertdelta.
212. Ellingsgaard, Óluva, 2007: Evaluation of wireline well logs from the borehole Kyrkheddinge-4 by comparsion to measured core data.
213. Åkerman, Jonas, 2007. Borrkärnekartering av en Zn-Ag-Pb-mineralisering vid Stenbränet, Västerbotten.
214. Kurlovich, Dzmitry, 2007: The Polotsk-Kurzeme and the Småland-Blekinge Deformation Zones of the East European Craton: geomorphology, architecture of the sedimentary cover and the crystalline basement.
215. Mikkelsen, Angelica, 2007: Relationer mellan grundvattenmagasin och geologiska strukturer i samband med tunnelborrning genom Hallandsås, Skåne.
216. Trondman, Anna-Kari, 2007: Stratigraphic studies of a Holocene sequence from Taniente Palet bog, Isla de los Estados, South America.
217. Månsson, Carl-Henrik & Siikanen, Jonas, 2007: Measuring techniques of Induced Polarization regarding data quality with an application on a test-site in Aarhus, Denmark and the tunnel construction at the Hallandsås Horst, Sweden.
218. Ohlsson, Erika, 2007: Classification of stony meteorites from north-west Africa and the Dhofar desert region in Oman.
219. Åkesson, Maria, 2008: Mud volcanoes - a review.
220. Randsalu, Linda, 2008: Holocene relative sea-level changes in the Tasiusaq area, southern Greenland, with focus on the Ta1 and Ta3 basins.
221. Fredh, Daniel, 2008: Holocene relative sea-level changes in the Tasiusaq area, southern Greenland, with focus on the Ta4 basin.
222. Anjar, Johanna, 2008: A sedimentological and stratigraphical study of Weichselian sediments in the Tvärkroken gravel pit, Idre, west-Central Sweden.

LUNDS UNIVERSITET

Geologiska institutionen
Gentrum för GeoBiosfärsvetenskap
Sölvegatan 12, 223 62 Lund